

1                   **Study on the Biological Communities and Bioweathering of the**  
2                   **Marble Surfaces of the Hall of Prayer for Good Harvests at the**  
3                   **Temple of Heaven (Beijing, China)**

4

5                   Youping Tian \*

6                   School of Earth Sciences and Resources, China University of Geosciences (Beijing), Beijing, China

7

8

9

10               **Abstract:** This study investigates the biological communities and bioweathering of the marble  
11               surfaces of the Hall of Prayer for Good Harvests at the Temple of Heaven in Beijing. The dominant  
12               organisms are aerophytic cyanobacteria, which thrive in calcareous environments, are drought-  
13               resistant, slow-growing, and highly resilient. These cyanobacteria exhibit different community  
14               compositions depending on the orientation of the marble surface. On east-facing, warm and humid  
15               surfaces, the communities are mainly composed of small filamentous cyanobacteria such as  
16               *Scytonema* sp.2 and coccoid cyanobacteria like *Gomphosphaeria* sp. On west-facing, hot and humid  
17               surfaces, the dominant organisms are *Scytonema* sp.1 (a small filamentous cyanobacterium) and  
18               mosses. On north-facing, cold and humid surfaces, the biological communities mainly consist of  
19               coccoid cyanobacteria such as *Myxosarcina* sp. and *Gomphosphaeria* sp. On south-facing, hot and  
20               dry surfaces, the communities are primarily made up of small or large filamentous cyanobacteria,  
21               including *Scytonema* sp.1 and *Nostoc* sp. The intensity of weathering observed varies by orientation:  
22               South > West > East > North. This pattern aligns with the observed "Cloud Chi Heads" weathering  
23               features on surfaces facing different directions. The biological communities on the marble surface  
24               display a range of colors, with gray-black being the most common, followed by gray-white, black,  
25               brown, and dark brown. The gray-black communities are mainly composed of *Myxosarcina* sp. and  
26               *Gomphosphaeria* sp. These communities also exhibit various morphologies, including membranous,

---

\* Corresponding author at: School of Earth Sciences and Resources, China University of Geosciences (Beijing), Beijing, China  
E-mail address: [typ@cugb.edu.cn](mailto:typ@cugb.edu.cn) (Y. Tian)

27 pilose, carpet-like, leathery, shell-like, and powdery layers. The species composition varies across  
28 these morphological types. The growth of aerophytic organisms on rock surfaces is controlled by  
29 macroscopic hydrodynamics and micro-topographical features. At the macro scale, in areas with  
30 low rainfall intensity, biofilms are sparse and biological weathering is weak. In areas with high  
31 rainfall, cyanobacteria-rich "ink bands" can form, leading to intense biological weathering. At the  
32 micro scale, micro-topographical features regulate local hydrological conditions and determine  
33 colonization patterns: rough, uneven surfaces and discrete water films promote spot-like bio-  
34 colonies that lead to solution pores and pits; linear decorations or joints with directional water  
35 retention drive linear biological growth, forming solution marks and grooves; smooth, dense  
36 surfaces with uniform water film coverage support planar microbial growth, ultimately resulting in  
37 overall layer separation from weathering. The mechanism of biological weathering involves the  
38 secretion of organic acids by aerophytic organisms. These acids dissolve inorganic salts in the rock,  
39 providing nutrients while gradually "eroding" the rock, damaging its surface structure, and leading  
40 to progressive weathering. Preventing or reducing the growth of aerophytic organisms is key to  
41 slowing the biological weathering of the stone relics on the Hall of Prayer for Good Harvests.

42

43

44 Keywords: The Hall of Prayer for Good Harvests, marble, aerophytic organisms, cyanobacteria,  
45 bioweathering

46

## 47 1. introduction

48

49 The Hall of Prayer for Good Harvest, located in the Temple of Heaven in Beijing, China,  
50 was completed in 1420. It served as the site for the emperors of the Ming and Qing dynasties to  
51 perform the "Heaven Worship" and "Prayer for Good Harvest" rituals. It is also the largest  
52 existing ancient architectural complex for heaven worship in the world. In 1961, the State  
53 Council of China designated the Temple of Heaven as a "National Key Cultural Relic Protection  
54 Unit." In 1998, it was recognized by UNESCO as a "World Cultural Heritage Site." The base  
55 of the Hall of Prayer for Good Harvests is a three-tiered circular platform made of white marble,  
56 6 meters high and surrounded by a balustrade (Fig. 1-a). The marble used in the construction is

57 divided into two types: White marble and Bluish-white marble. White marble, due to its fine  
58 texture and ease of detailed carving, is often used in decorative parts such as balustrades and  
59 carvings. Bluish-white marble, with its higher compressive strength (Ye and Zhang, 2019) and  
60 better corrosion resistance compared to White marble (Qu, 2018), is typically used in load-  
61 bearing and wear-resistant areas such as the base and paving. Most of the White marble and  
62 Bluish-white marble used in the construction come from the marble quarries in Dashiwo Town,  
63 Fangshan District, Beijing. (Wu and Liu, 1996; Lü and Wei, 2020). Compared to other types of  
64 rock used in the Temple of Heaven complex (such as limestone, granite, and sandstone), the  
65 marble used in the Hall of Prayer for Good Harvests is the most susceptible to weathering due  
66 to its lower hardness. White marble, a special variety of marble, is particularly sensitive to  
67 weathering (Ye and Zhang, 2019). Additionally, because marble is rich in calcium, it serves as  
68 a preferred substrate for biological growth (Miller, et al., 2006). However, the organisms are  
69 not uniformly distributed across the entire marble surface; their distribution is selective. In  
70 addition to requiring a calcium-rich substrate, they also need water. In areas with low rainfall  
71 intensity (such as high and protruding locations on the marble surface), where water is scarce,  
72 there is little to no biological growth, and the surface appears white or yellowish-white with  
73 minimal biofilm and weak bioweathering. In contrast, in areas with high rainfall intensity (such  
74 as water convergence points, channels, and Chi Heads), where water is abundant, there is  
75 extensive biological growth, and the surface appears black (with patches of brown and gray-  
76 black) with a prominent biofilm and strong bioweathering. (Fig.1-b). The gradient distribution  
77 of the biofilm on the rock surface is significantly spatially coupled with the variations in  
78 instantaneous runoff, reflecting an optimal water allocation mechanism in arid environments  
79 (Tian, 2004; Macedo, et al., 2009). In addition to the rock substrate and precipitation,  
80 environmental factors such as wind and air pollution also influence microbial colonization, a  
81 phenomenon known as "bioreceptivity" of vulnerable structural materials (Guillitte and  
82 Dreesen, 1995; Miller, et al., 2012). Among these organisms, cyanobacteria are particularly  
83 significant because they can grow with just light and water, and they can survive within the  
84 rock, playing a crucial role in the degradation of stone cultural relics (C., Gaylarde, 2020).

85

86



a

b

87 **Fig. 1.** The hall of Prayer for Good Harvests in the Temple of Heaven, Beijing, China, and  
 88 the distribution of black biofilm on its marble surface.

89 a. The Hall of Prayer for Good Harvests has a base consisting of three tiers of marble platforms; b The surface of marble platforms is  
 90 covered with black biofilm, which is distributed according to the intensity of rainfall. In areas with low rainfall intensity, the biofilm is not  
 91 noticeable. In areas with high rainfall intensity (such as channels, water convergence points, and Chi Heads), there is a significant  
 92 distribution of black biofilm.

93

94 Black microbial distributions, forming black crusts, have been observed on marble surfaces in  
 95 many regions (Checcucci, et al., 2022; Monte and Sabbioni, 1986; Praderio, et al., 1993; Gorbushina,  
 96 et al., 2002). This phenomenon is also referred to as marble blackening (Moropoulou, et al., 1998),  
 97 bioweathering, or biodeterioration. The microbial communities on marble surfaces exhibit high  
 98 diversity (Timoncini et al., 2022). The black crust microbial communities are primarily composed  
 99 of coccoid and filamentous cyanobacteria from the genera *Chroococcus*, *Gloeocapsa*, and  
 100 *Tolypothrix* (Lombardozzi, et al., 2012), as well as green algae, fungi (Isola, et al., 2016; Leo, et al.,  
 101 2019; Marvasti, et al., 2012), and lichens (Pinna, et al., 2018). *Chroococcus* can bore into the marble  
 102 surface, demonstrating remarkable environmental adaptability: not only do they form blue-green  
 103 biofilms on the rock surface (epilithic growth), but they also penetrate through cracks  
 104 (chamomelitic growth), colonize mineral interstices (cryptoendolithic growth), and even  
 105 actively excavate (euendolithic growth) deeper into the marble. The tubular tunnels drilled by  
 106 *Chroococcus* in calcite crystals involve both chemical dissolution and mechanical erosion, making  
 107 them a dominant species in the community (Golubić, et al., 2015; Scheerer, et al., 2009). Biofilms

108 alter the thermal and moisture properties of the material, exert colloidal mechanical stress, and  
109 secrete acidic and redox metabolites, which intensify mineral lattice destruction and promote the  
110 formation of harmful crusts (Guiamet, et al., 2013; Warscheid and Braams, 2000). They can also  
111 accelerate rock weathering, leading to the formation of pits (Danin and Caneva, 1990) and control  
112 the micro- and macro-morphology of the rock surface (Tian, 2004). Black biofilms on marble  
113 surfaces show differential erosion based on orientation, such as differences between windward and  
114 leeward faces (Danin and Caneva, 1990). Height differences also play a role, with height having a  
115 greater impact on microbial weathering than orientation. The microenvironmental gradients on the  
116 rock surface are the core driving factors for the biological erosion of stone cultural heritage (Trovão  
117 and Portugal, 2024). In extremely arid environments, "gravel shell" microbial communities  
118 composed of lichens, cyanobacteria, and fungi drive the decomposition of rock particles and the  
119 formation of primitive soil (terrestrial protopedon) through bioweathering mechanisms such as pH  
120 changes, swelling and shrinking, enzymatic activity, and mineral migration (Jung, et al., 2020). Even  
121 in areas with fewer black biofilms, the frequency of microbial presence increases as the physical  
122 and chemical acid erosion of marble forms a powdery layer, accelerating the transformation of  
123 marble into soil and posing a serious threat to marble cultural heritage. Understanding the  
124 bioweathering patterns on marble surfaces is crucial for the conservation of marble cultural heritage.  
125 For example, targeted use of microbial methods to remove black crusts can be more effective than  
126 purely chemical or laser methods (Gioventù, et al., 2011).

127 Current research on the weathering of marble cultural heritage in Beijing has primarily focused  
128 on the roles of physical and inorganic chemical processes, such as acid erosion. Studies have found  
129 that the surface peeling and pollution of the marble steles at the Confucian Temple in Beijing are  
130 caused by acid rain erosion (He, 2021). Freeze-thaw cycles can lead to internal structural damage  
131 in rocks, while salt fog crystallization causes pore expansion and degradation (Li, 2023).  
132 Temperature changes affect the physical and mechanical properties of dolomitic marble in Beijing,  
133 leading to surface peeling, dissolution of dolomite crystals, and the formation of crusts due to SO<sub>2</sub>  
134 and dust pollution (Liu, 2020; Zhang, et al., 2016; Wang, et al., 2022). The mechanism of granular  
135 peeling on marble surfaces is attributed to the low amount of cementing material between particles,  
136 resulting in weak cementation. Surface particles are disrupted by mining unloading, processing  
137 damage, stress concentration, and temperature variations, leading to peeling (Wang, 2010).

138 Temperature fluctuations, acid rain dissolution, water erosion, and salt micro-crack filling are the  
139 main causes of weathering in Fangshan marble in Beijing (Zhang, et al., 2015). Research on the  
140 weathering of white marble components in the Hall of Supreme Harmony in the Forbidden City  
141 indicates that thermal stress from solar radiation and rain erosion are the primary factors (Wu, et al.,  
142 2023). It has been found that under the combined action of acid and salt, dolomite crystals degrade  
143 through dissolution, interstitial erosion, and spalling. Salt crystallization accelerates the latter two  
144 types of damage, while acid erosion promotes salt penetration, significantly increasing the rate of  
145 degradation (Zheng, et al., 2025). Regarding bioweathering of marble in Beijing, only a few studies  
146 have mentioned it (Beijing Institute of Ancient Architecture, 2018). The main types of damage to  
147 marble in Beijing include fissures, peeling, disintegration, crust formation, solution pits, erosion,  
148 component loss, discoloration, biological parasitism, and improper human restoration (Yang, 2016).  
149 Two types of peeling in white marble in the Beijing area have been identified: one driven by the  
150 synergistic effects of thermal weathering, lichen, and rainfall, and the other by acid rain and capillary  
151 water absorption (Zhang, 2022). To understand the patterns of bioweathering in marble, it is  
152 essential to know the composition, structure, and metabolic potential of the resident microbial  
153 communities and their interactions with the stone (Pinna, 2017; Marvasti, et al., 2019). This study  
154 focuses on analyzing the community composition, structure, and relative biomass of biofilms on the  
155 marble surface of the Hall of Prayer for Good Harvests in Beijing. By identifying the development  
156 process and patterns of the biofilm communities, we aim to reveal the mechanisms of biocorrosion  
157 and provide a scientific basis for developing more targeted conservation strategies for marble  
158 cultural heritage.

159

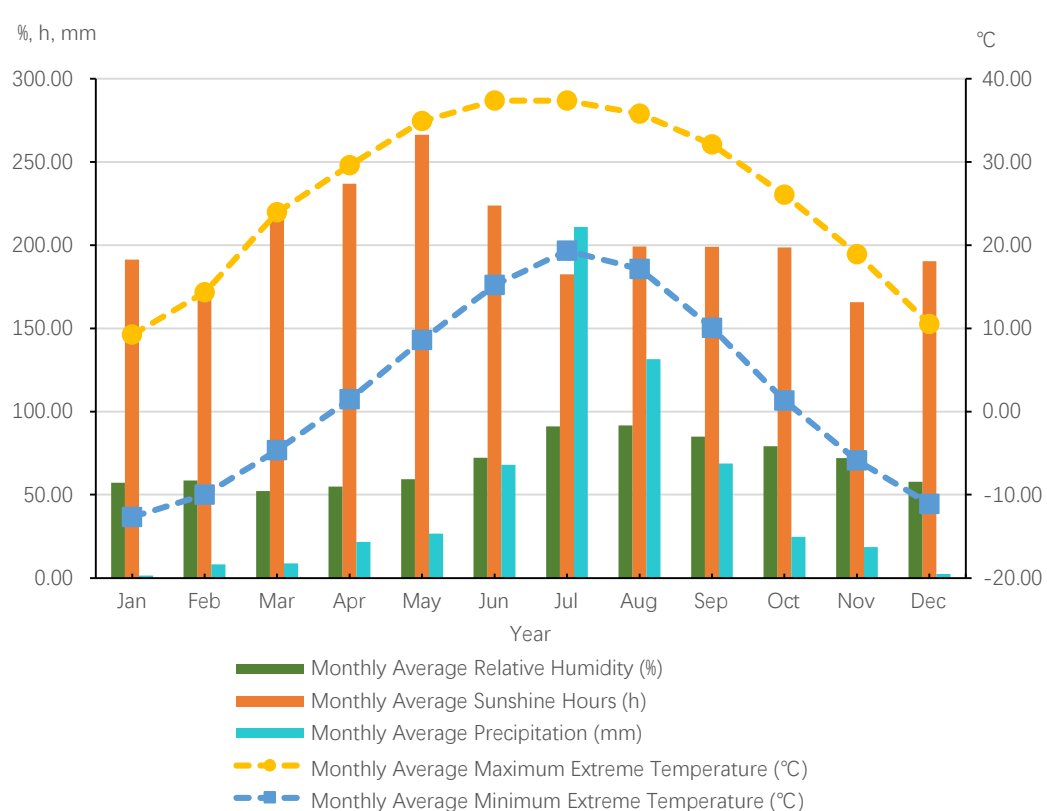
## 160 1. Overview of the Study Area

161

162 Beijing is located in a warm temperate monsoon semi-humid climate zone, characterized by a  
163 cool mountain climate. The region has an average annual temperature of 10.8°C, with a frost-free  
164 period of approximately 150 days. In winter, Beijing is influenced by cold air masses from the  
165 northwest, resulting in a cold and dry climate. The prevailing wind direction during this season is  
166 from the northwest, with an average annual wind speed of 1.9 meters per second. In summer, the  
167 influence of the subtropical high-pressure system makes the climate hot, and rainfall is relatively

168 concentrated, especially from July to September, when about 85% of the annual precipitation occurs,  
169 often in the form of heavy rain. Autumn in Beijing is generally pleasant, while spring is relatively  
170 short. The frost-free period ranges from 190 to 200 days. Under extreme weather conditions, the  
171 maximum summer temperature can reach 42°C, and the minimum winter temperature can drop to -  
172 25°C. According to data from the National Meteorological Information Center of Beijing from 2009  
173 to 2024, the annual precipitation in Beijing shows significant fluctuations (Fig. 2). There is no clear  
174 trend in the annual average relative humidity and annual average precipitation, but there is an  
175 increasing trend in the annual average sunshine hours and annual average extreme maximum  
176 temperature, and a decreasing trend in the annual average extreme minimum temperature (Fig. 3).  
177 During the period from 2009 to 2024, the multi-year average annual total rainfall was 610 mm.

178

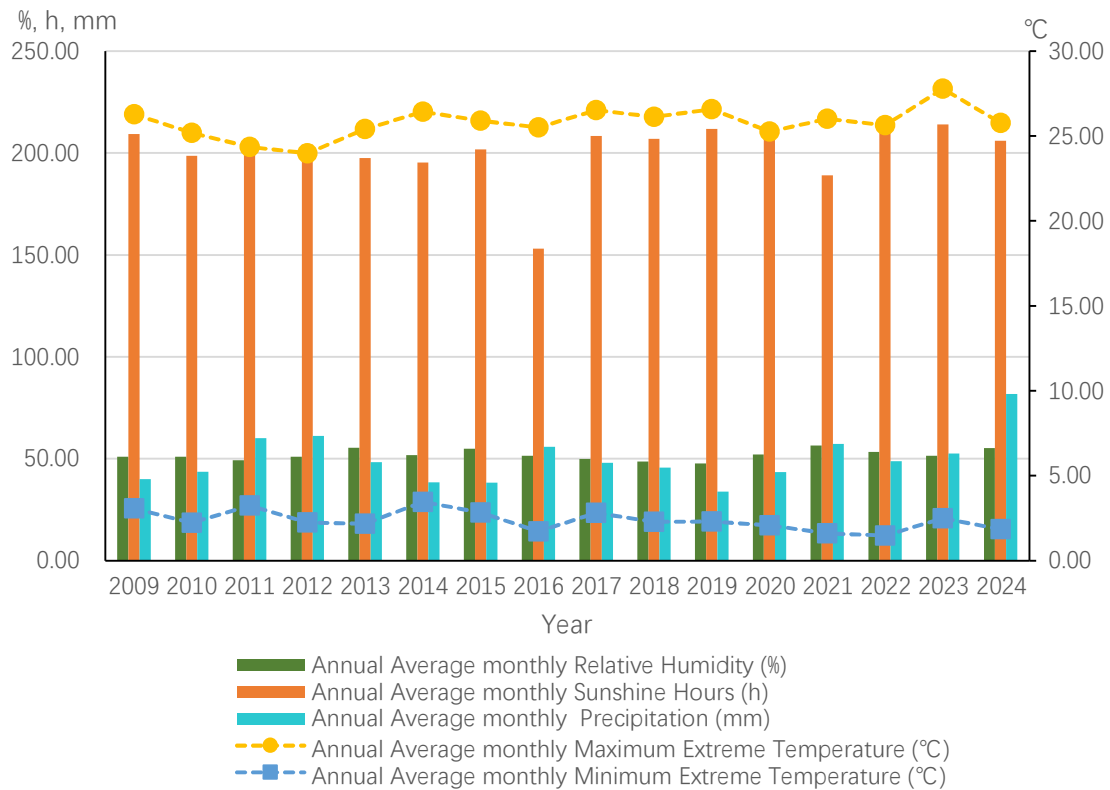


179

180

181 Fig. 2 Monthly average relative humidity, monthly average sunshine hours, monthly average precipitation,  
182 monthly average extreme maximum temperature, and monthly average extreme minimum temperature  
183 in the Beijing region from 2009 to 2024

184 (based on data from the National Meteorological Science Data Center Website).



187 Fig. 3 Annual average relative humidity, annual average sunshine hours, annual average precipitation, annual average extreme maximum temperature, and annual average extreme minimum temperature in the Beijing region from 2009 to 2024

190 (based on data from the National Meteorological Science Data Center Website).

193 The base of the Hall of Prayer for Good Harvests at the Temple of Heaven is divided into three  
 194 tiers (Fig. 1-a). Each tier of its white marble base is adorned with 100 intricately carved Chi Heads  
 195 (Fig. 1-b, Fig. 16). The Chi Head (Chi Shou) is a unique functional and decorative architectural  
 196 element in traditional Chinese architecture, inspired by the mythical hornless dragon-like creature  
 197 "chi" Resembling a dragon's head without horns, it is commonly found on the roofs, beams, columns,  
 198 and stone railings of palaces and temples. Its design integrates both aesthetics and practicality:  
 199 rainwater is channeled through hidden drainage holes in the Chi Heads, preventing water erosion of  
 200 the base while creating a distinctive visual effect. The three tiers of the altar collectively have a total  
 201 of 300 Chi Heads, with the decorative themes progressively layered—dragon heads (Dragon Chi

202 Heads) on the upper tier symbolize imperial authority, phoenix heads (Phoenix Chi Heads) on the  
203 middle tier represent auspicious harmony, and cloud patterns (Cloud Chi Heads) on the lower tier  
204 reflect the connection between heaven and earth. During the rainy season, water cascades from the  
205 mouths of the Chi Heads on all three tiers, creating a spectacular sight of "dragons spouting torrents,  
206 phoenixes holding pearls, and clouds rolling like waves." Over time, the weathering of the Chi  
207 Heads has varied significantly depending on their orientation (Fig. 16), vividly illustrating the  
208 dynamic interaction between ancient architectural elements and the natural environment.

209 The main production area for Beijing marble is Dashiwo Town, located in the southwestern  
210 part of Fangshan District, Beijing. In the distribution of marble layers in Fangshan, Bluish-white  
211 marble is the first to be quarried due to its shallow burial depth. On the other hand, White marble is  
212 found in the deepest layer, with a burial depth that is usually the deepest among the stone layers,  
213 ranging from 90 cm to 150 cm in thickness. In the construction industry, both White marble and  
214 Bluish-white marble are widely used as marble materials.

215

## 216 2 Research Methods

### 217 2.1 Field Work

218 Different forms of biofilm communities on the marble surface were collected (biofilms are  
219 loose and easily detachable, so a small amount was gently picked by hand without damaging the  
220 cultural relics), placed in specimen boxes, numbered, and photographed. The appearance, color, and  
221 morphology of the biofilms were described, and the date and location were recorded. The micro-  
222 morphologies formed by the dissolution of the biofilm communities were observed and  
223 photographed. A total of 40 biofilm community specimens were collected, and 22 photographs of  
224 the field biofilm communities were taken. On clear, sunny days, the surface temperature of the rock  
225 in the sampling area was measured using an infrared thermometer (DL333380, Deli, China). At the  
226 same time, the degree of weathering of the Chi Heads was marked on the overhead view of the Hall  
227 of Prayer for Good Harvests. Chi Heads with complete surface ornamentation were marked in green,  
228 those with incomplete ornamentation were marked in yellow, and those with completely weathered  
229 and disappeared ornamentation were marked in red. Environmental humidity in different directions  
230 was measured using a hygrometer (THM-H1, Delixi, China).

231

232 2.2 Laboratory Work

233 2.2.1 Microscopic Observation

234 The size, morphology, and color of the biofilm communities were observed using a  
235 stereomicroscope (Szx7, Olympus, Japan). Then, temporary slides were prepared from different  
236 colored biofilm communities and observed under a biological microscope (Bx51, Olympus, Japan).  
237 The species of the biofilm communities were identified (Desikachary, 1959; Geitler, 1932; Komarek,  
238 1998, 2005, 2013; Zhu, 1991; Fott, 1980; Hu and Wei, 2006), and photographs were taken. For each  
239 biofilm community ecological specimen, a microslide was prepared, resulting in a total of 40  
240 microslides, and 142 microscopic photographs were taken.

241 2.2.2 Biomass Statistics

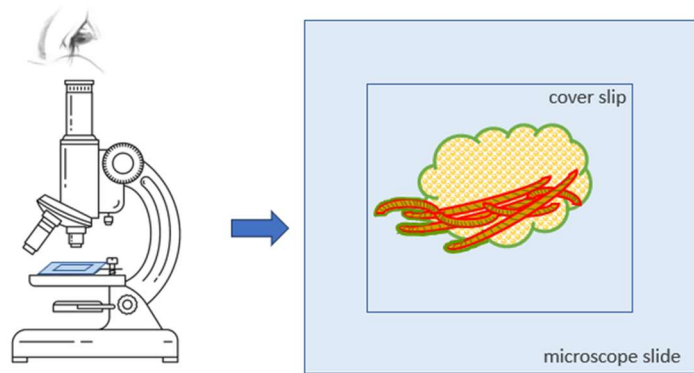
242 The volume percentage of the species in the biofilm communities was recorded. The volume  
243 percentages of the species were statistically analyzed to calculate the relative volume ( $V_x$ , relative  
244 biomass) and the relative volume percentage ( $Y_x$ , relative biomass percentage). The statistical and  
245 calculation methods are as follows:

246 (1) Relative Volume ( $V_x$ , Relative Biomass)

247 To obtain the relative volume, the following steps need to be taken:

248 1) Determine the volume percentage ( $v(x)\%$ )

249 By estimating the percentage of the volume that each species occupies relative to the total  
250 volume of all species in each microslide, the volume percentage ( $v(x)\%$ ) of that species in the  
251 microslide is obtained. The estimation can be based on the area occupied by each species in the  
252 microslide, as within the same microslide, the thickness between the cover slip and the slide is nearly  
253 uniform across different areas. Therefore, under the same thickness, the larger the area occupied by  
254 a species, the greater its volume (Fig. 4).

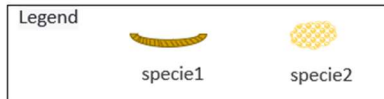


$$V(\text{Specie1})\% = \frac{\text{specie1 area} \times \text{high}}{(\text{specie1 area} + \text{specie2 area}) \times \text{high}} \times 100 \%$$

$V(\text{Specie1})\%$ : volume percentage of specie1

area within the red line: specie1 area

area within the green line: specie1 area + specie2 area



255

256 Fig. 4 Visual Method for the volume percentage ( $v(x)\%$ ) of a Specie  
257 in a Biofilm Community Microslide

258 If there are two species in the microslide: Species 1 and Species 2, the volume percentage of Species 1 can be estimated by dividing the  
259 area occupied by Species 1 by the total area occupied by both Species 1 and Species 2, and then multiplying by 100. This gives the volume  
260 percentage ( $v(x)\%$ ) of Species 1 in the microslide.

261

262 2) Sum the Volume Percentages

263 Add up the volume percentages of the same species across all microslides in the study area to  
264 obtain the relative volume ( $Vx$ ) of a species in the study area. The relative volume of a species  
265 roughly reflects its relative biomass in the biofilm community of the study area. It does not represent  
266 the actual volume but is an estimated relative value that is meaningful for comparison.

267

$$268 Vx = v(x)_{i_1} + v(x)_{i_2} + \dots + v(x)_{i_x}$$

269  $i_x$  is the microslide number;  $x$  is a specific species ( $x=a, b, c, \dots$ );  $v(x)_{i_x}\%$  is the volume percentage of  
270 species  $x$ .

271 (2) Relative Volume Percentage ( $Yx$ , Relative Biomass Percentage)

272 This is the percentage of the relative volume ( $Vx$ ) of a species in the biofilm community of the

273 study area relative to the sum of the relative volumes of all species in the biofilm community. It is  
274 also referred to as the relative biomass percentage.

275

276 
$$Y_x = \frac{V_x}{n \times 100} \times 100\%$$

277 n is the total number of microslides.

278

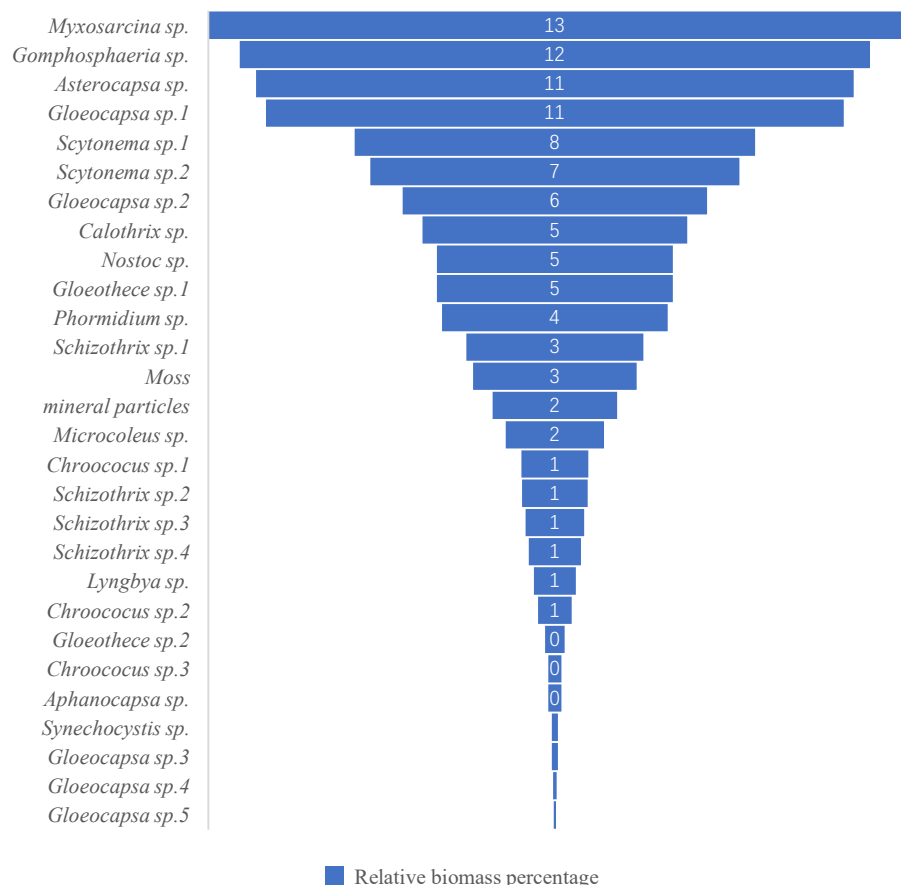
279 The relative volume percentage, also known as the relative biomass percentage, does not  
280 represent the actual biomass. This is because it is currently very difficult to accurately measure the  
281 biomass of biofilm communities on marble rock surfaces. By estimating through microscopic  
282 observation, one can get a rough understanding of the growth status of the biofilm community. It is  
283 a relative value and is meaningful only for comparative purposes.

284

285 3 Results

286 3.1 Distribution of communities in the Study Area

287 The composition of the biofilm communities on the marble surface in the study area includes  
288 a total of 30 genera and species (Fig. 5). The most abundant species is *Myxosarcina* sp., followed  
289 by *Gomphosphaeria* sp., *Asterocapsa* sp., *Gloeocapsa* sp.1 (Fig. 6), and *Scytonema* sp.1, among  
290 others.



■ Relative biomass percentage

291

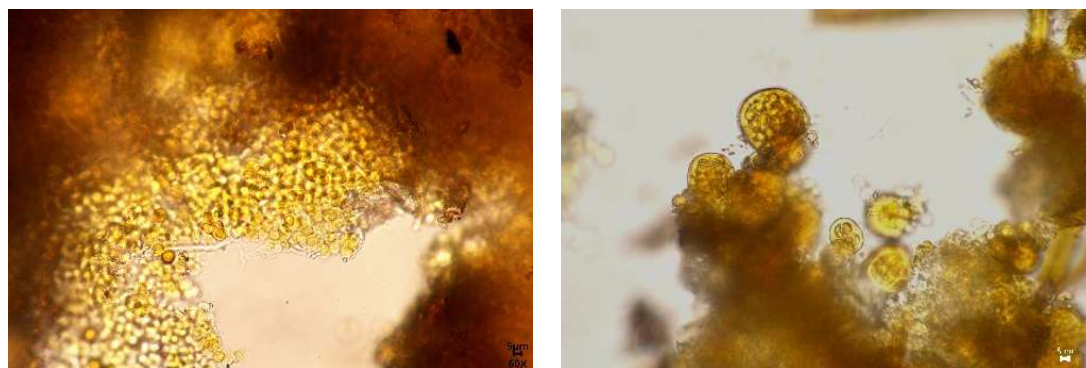
292

Fig. 5. Relative biomass percentage of marble surface of the Hall of Prayer for Good Harvests

293

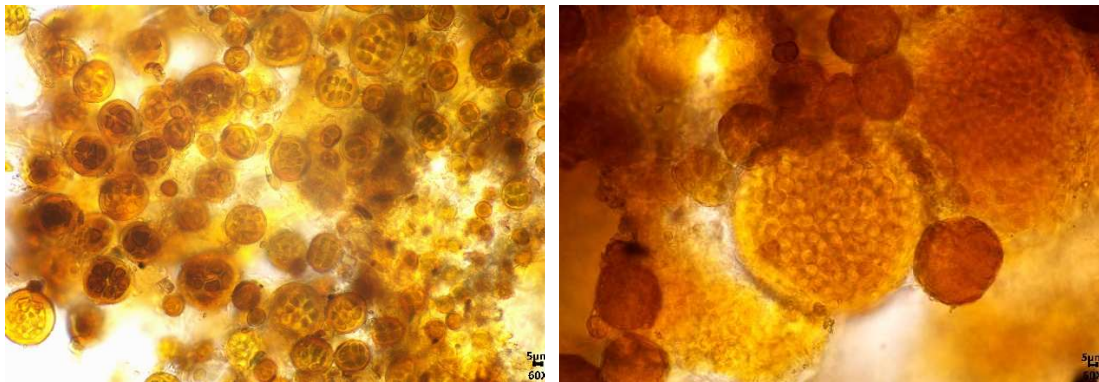
in the Temple of Heaven, Beijing, China.

294



a. *Myxosarcina* sp.

b. *Gomphosphaeria* sp.



c. *Asterocapsa* sp.

d. *Gloeocapsa* sp.1

295 **Fig. 6.** Dominant organisms on the marble surface of the Hall of Prayer for Good Harvests  
 296 in the Temple of Heaven, Beijing., China.  
 297

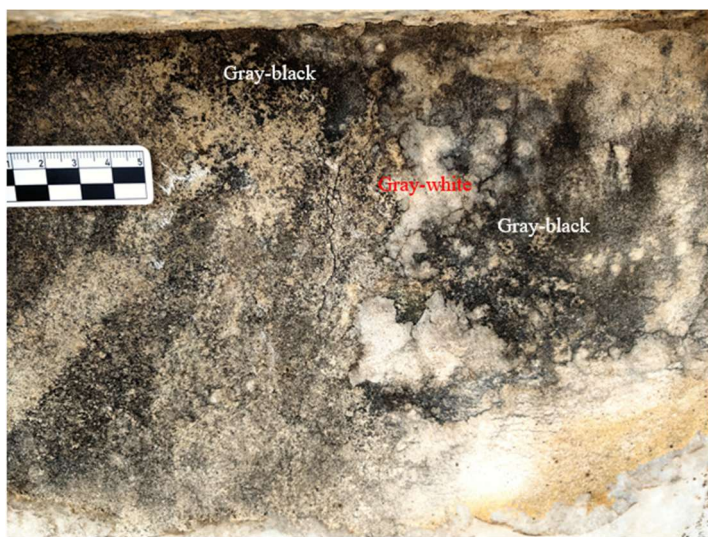
298 3.2 Characteristics of the distribution of biological communities on marble surfaces with  
 299 different orientations in the study area

300 The Hall of Prayer for Good Harvests at the Temple of Heaven is a circular building (Fig. 16).  
 301 The marble surfaces facing different directions receive varying amounts of sunlight. The south-  
 302 facing surface receives the most sunlight, followed by the east and west-facing surfaces, which  
 303 receive sunlight for half a day. The north-facing surface is shaded and receives no direct sunlight.  
 304 This variation in sunlight exposure leads to differences in the biological populations on the rock  
 305 surfaces. The details are discussed below:

306  
 307 3.2.1 Characteristics of Biological communities on East-Facing Rock Surfaces

308 The biological communities on east-facing rock surfaces are primarily characterized by gray-  
 309 white, gray-brown, brown, gray-black, black-brown, white, and black-brown leathery appearances.  
 310 The main species include *Scytonema* sp.2, *Chlorococcum* sp., *Gloeocapsa* sp.2, *Gloeothece* sp.1,  
 311 *Myxosarcina* sp., *Phormidium* sp., *Calothrix* sp., *Gloeothece* sp.2, *Lyngbya* sp., *Gloeocapsa* sp.5,  
 312 and *Chroococcus* sp.1 (Fig.7) . Among these, the dominant species are *Scytonema* sp.2,  
 313 *Chlorococcum* sp., accounting for 25% and 23% of the relative biomass percentage (Fig. 8) .

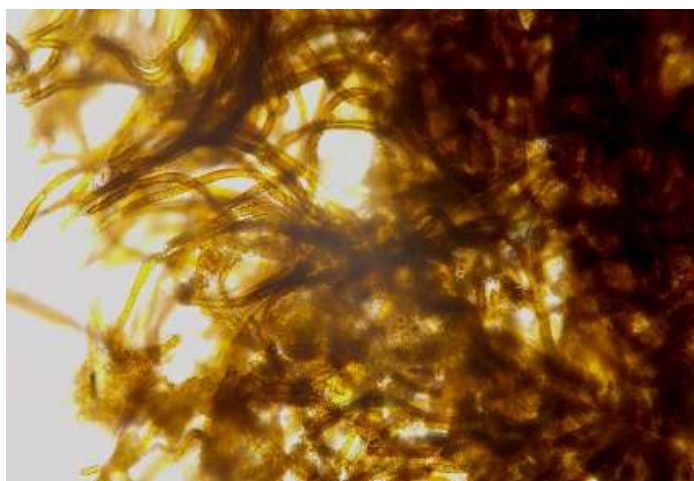
314  
 315



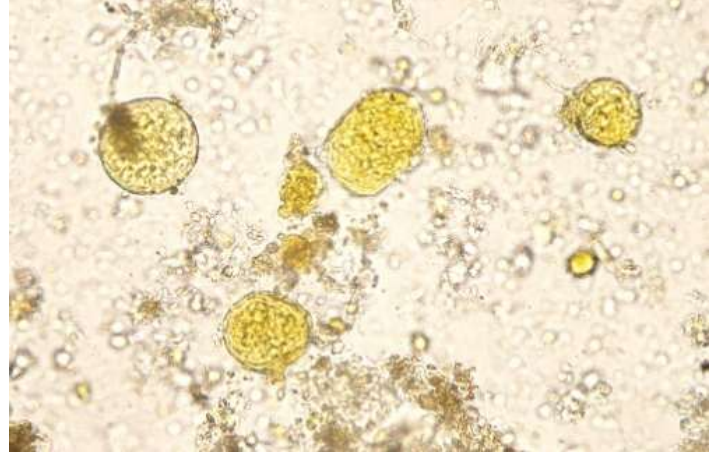
a. Gray-white, Gray-black



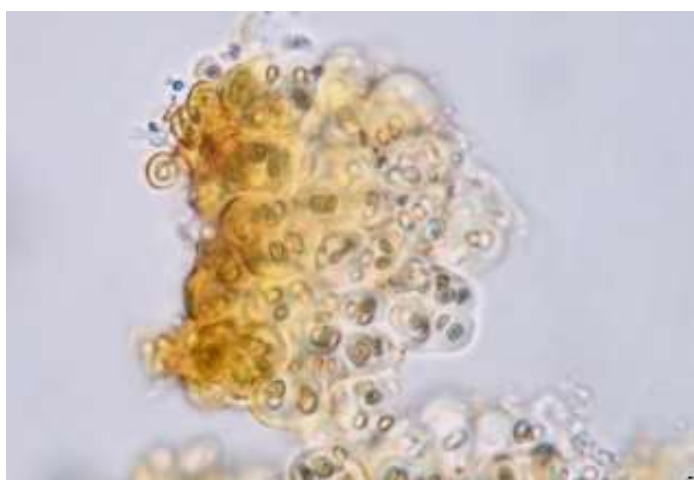
b. Gray-white, Gray-brown, Black-brown, White



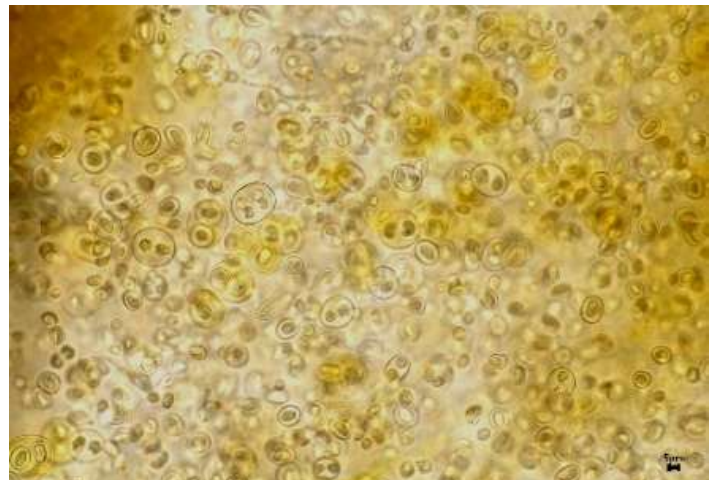
c. *Scytonema* sp.2



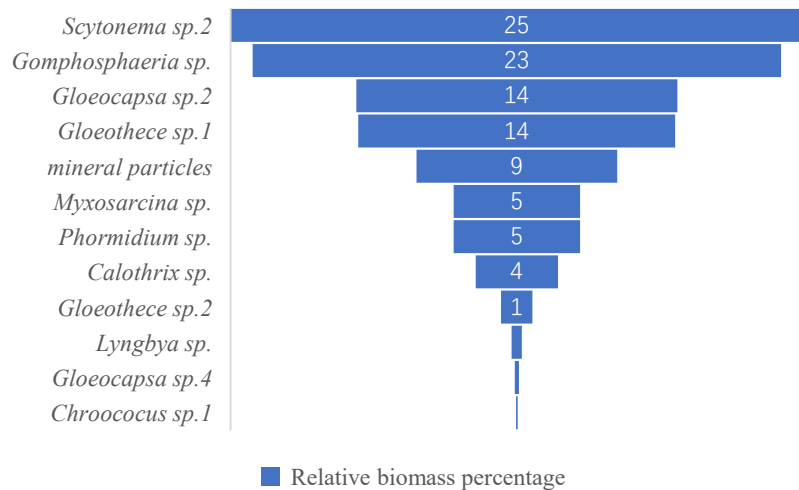
d. *Gomphosphaeria* sp.



e. *Gloeocapsa* sp.2



f. *Gloeothecae* sp.1



318

319

**Fig.8.** Biological population relative biomass percentage on the east-facing marble surface of the altar of

320

Prayer for Good Harvest in the Temple of Heaven, Beijing, China.

321

### 322 3.2.2 Characteristics of Biological communities on West-facing Rock Surfaces

323

The biological communities on west-facing rock surfaces are primarily characterized by black hairy, black membranous, yellow-green leathery, gray-black leathery, yellow-green, brown, and gray-green appearances. The main species include *Scytonema* sp.1, mosses, *Schizothrix* sp.1, *Myxosarcina* sp., *Asterocapsa* sp., *Gloeocapsa* sp.1, *Gomphosphaeria* sp., and *Gloeocapsa* sp.2 et al (Fig. 9) . Among these, the dominant species are *Scytonema* sp.1 and mosses et al, accounting for 28% and 20% of the relative biomass percentage respectively (Fig. 10) .

329





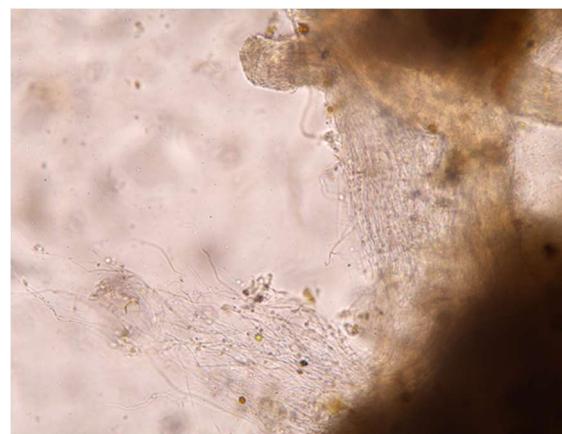
c. Yellow-green, Gray-green, Brown



d. *Scytonema* sp.1



e. moss

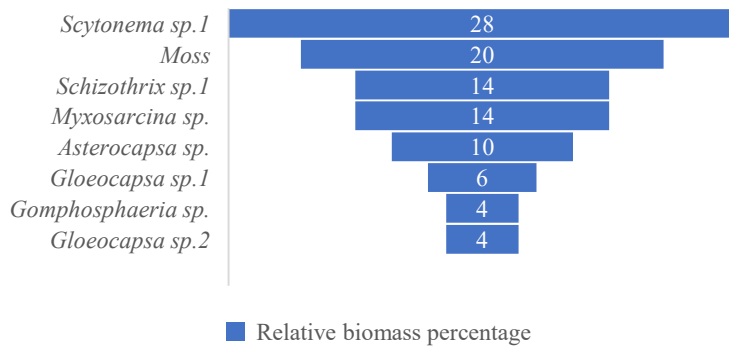


f. *Schizothrix* sp.1

330 **Fig. 9.** Micrographs of biomes and some species on the west-facing marble surface of the altar of

331 Prayer for Good Harvest in the Temple of Heaven, Beijing, China.

332



333

334

335 **Fig. 10.** Biological population relative biomass percentage on the west facing marble surface of the altar of

336 Prayer for Good Harvest in the Temple of Heaven, Beijing, China.

337 3.2.3 Characteristics of communities Distribution on North-facing Surfaces

338 The biological communities on north-facing rock surfaces are primarily characterized by gray-  
339 brown membranous, brown, gray-black, yellow-green, black-brown, gray-white, brown crusty,  
340 brown carpet-like, brown-black leathery, and brown-black membranous appearances. The main  
341 species include *Myxosarcina* sp., *Gomphosphaeria* sp., *Gloeocapsa* sp.1, *Schizothrix* sp.1,  
342 *Asterocapsa* sp., *Scytonema* sp.1, *Calothrix* sp., mosses, *Gloeocapsa* sp.2, *Microcoleus* sp.,  
343 *Chroococcus* sp., *Gloeothecae* sp.1, *Lyngbya* sp., *Gloeocapsa* sp., *Scytonema* sp.2, and *Synechocystis*  
344 sp. et al (Fig. 11) . Among these, the dominant species are *Myxosarcina* sp. and *Gomphosphaeria*  
345 sp., accounting for 17% and 15% of the relative biomass percentage respectively ( Fig. 12) .

346

347



a. Gray-brown membranous



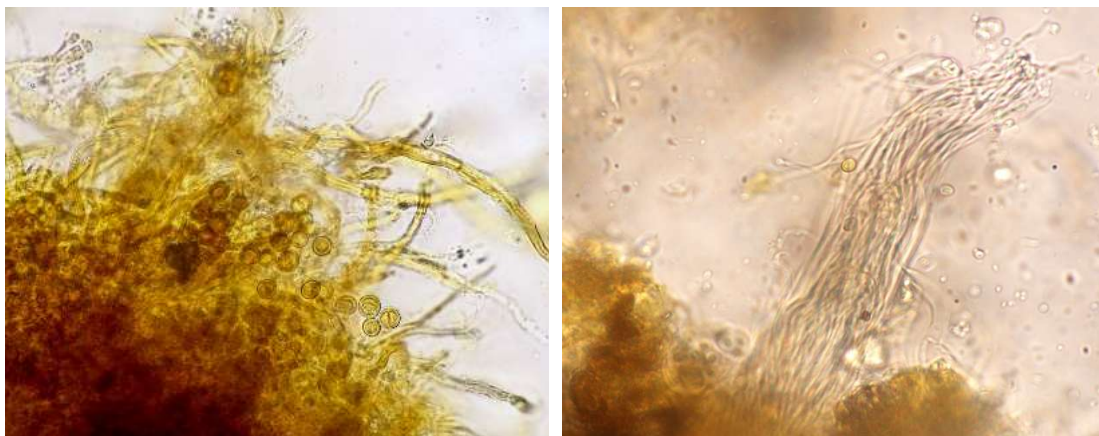
b. Gray-black



c. Yellow-green



d. Gray-white

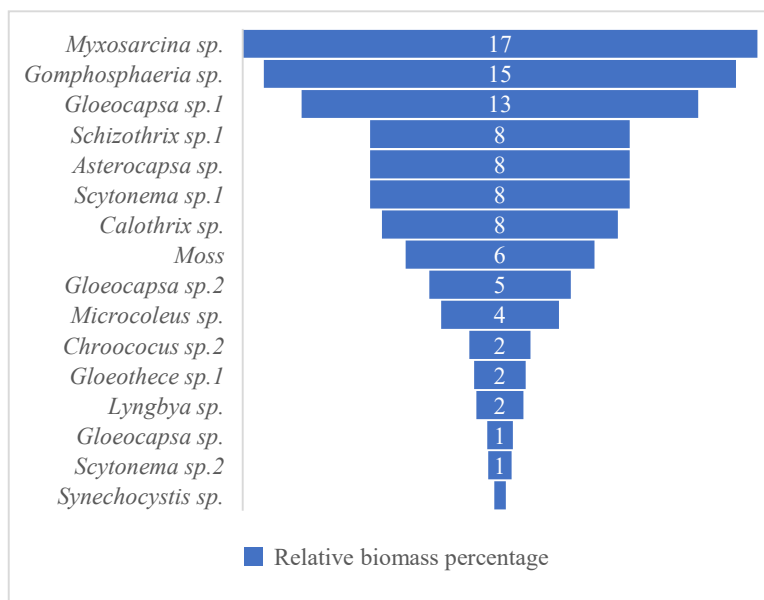


e. *Calothrix* sp.

f. *Microcoleus* sp.

348 **Fig. 11.** Micrograph of biological communities and some species on the north facing marble surface of the altar of  
 349 Prayer for Good Harvest in the Temple of Heaven, Beijing, China.

350



351

352

353 **Fig. 12.** Relative biomass percentage of biological population on the north facing marble surface of the altar of  
 354 Prayer for Good Harvest in the Temple of Heaven, Beijing, China.

355

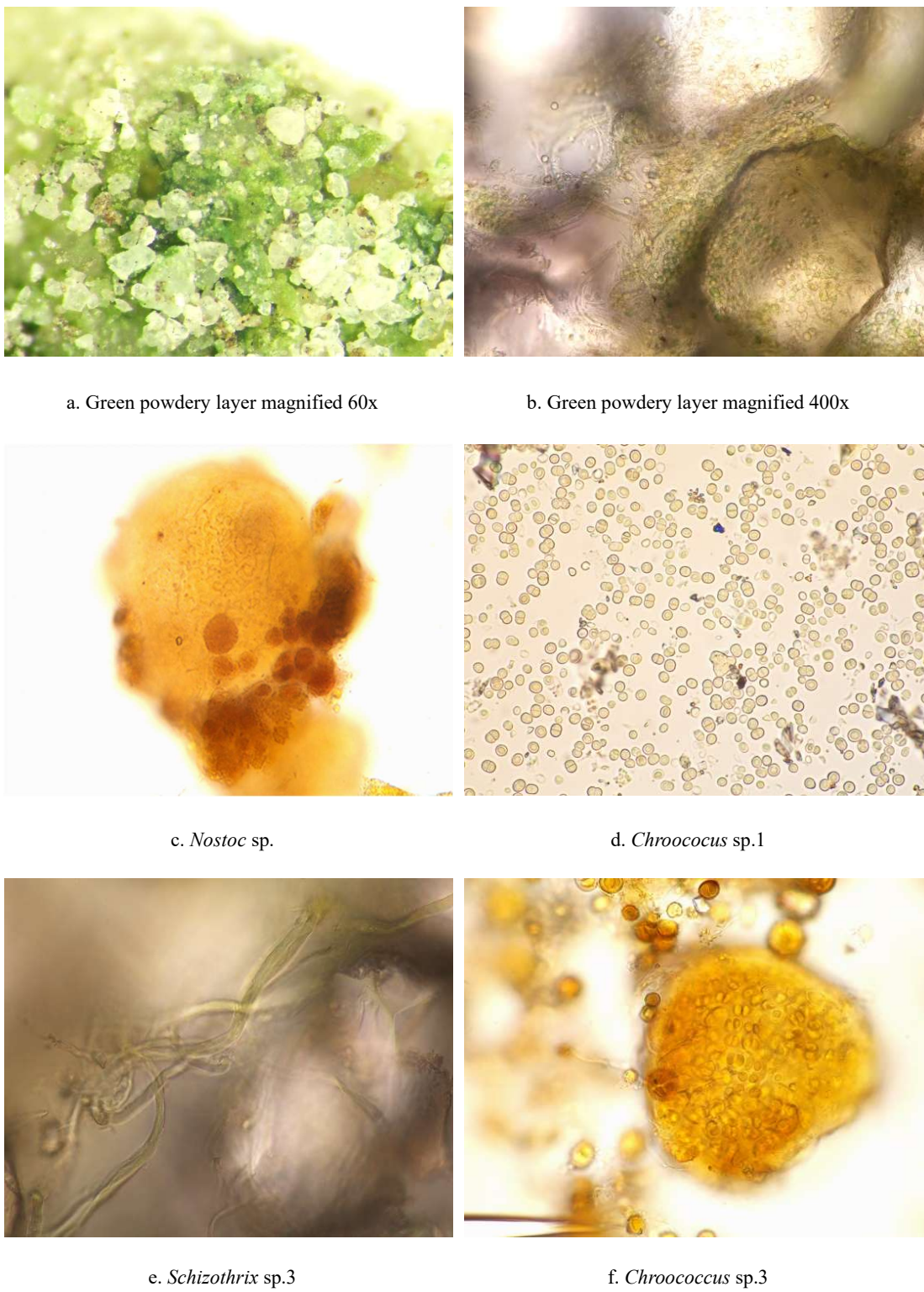
### 356 3.2.4 Characteristics of communities Distribution on South-facing Surfaces

357 The biological communities on south-facing rock surfaces are primarily characterized by gray-  
 358 green leathery, gray-white, gray-black membranous, black leathery, gray-black, brown-yellow, and  
 359 green powdery layer appearances. The main species include *Scytonema* sp.1, *Nostoc* sp.,

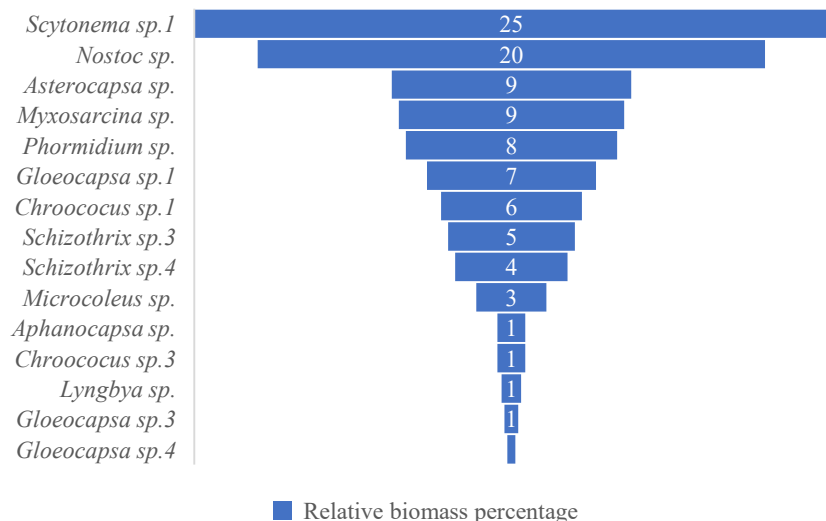
360 *Asterocapsa* sp., *Myxosarcina* sp., *Phormidium* sp., *Gloeocapsa* sp.1, *Chroococcus* sp.1, *Schizothrix*  
361 sp.4, *Microcoleus* sp., *Aphanocapsa* sp., *Chroococcus* sp.3, *Lyngbya* sp., *Gloeocapsa* sp.3, and  
362 *Gloeocapsa* sp.4 et al (Fig. 14) . Among these, the dominant species are *Scytonema* sp.1 and *Nostoc*  
363 sp., accounting for 25% and 20% of the relative biomass percentage respectively (Fig. 15) .



364 **Fig. 13.** Field photo of biomes on the south facing marble surface of the altar of  
365 Prayer for Good Harvest in the Temple of Heaven, Beijing, China.  
366  
367



368      **Fig. 14.** Micrograph of biomes and some species on the south facing marble surface of the altar of  
 369      Prayer for Good Harvest in the Temple of Heaven, Beijing, China.  
 370  
 371



372

373

374 **Fig. 15.** Biological population relative biomass percentage on the south facing marble surface of the altar of  
375 Prayer for Good Harvest in the Temple of Heaven, Beijing, China.

376

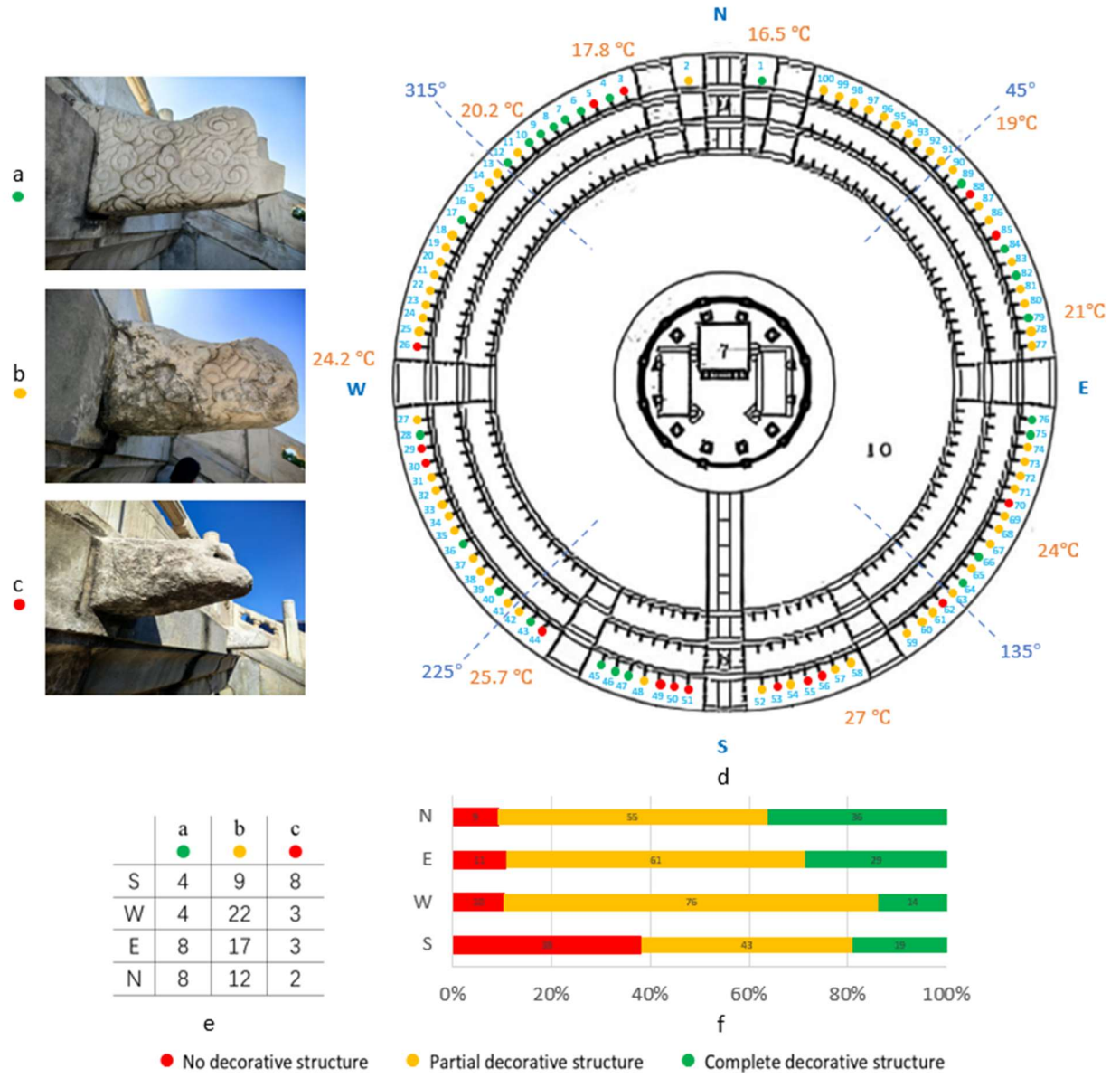
377 3.2.5 Comparison of communities on Different Orientations

378 The main aerophytic organisms on the rock surfaces include spherical cyanobacteria, small  
379 filamentous cyanobacteria, and large filamentous cyanobacteria. Their distribution is primarily  
380 influenced by the looseness of the substrate, sunlight, and moisture. From spherical cyanobacteria  
381 to small filamentous cyanobacteria and then to large filamentous cyanobacteria, the requirement for  
382 substrate looseness increases, the need for moisture decreases, and the requirement for sunlight  
383 duration increases. Mosses, on the other hand, prefer shady and moist environments.

384 Although both the east and west-facing surfaces of the Hall of Prayer for Good Harvests in the  
385 Temple of Heaven receive sunlight for half a day (Table 1), the east-facing surface receives sunlight  
386 in the morning when the rock surface temperature is lower. Even with sufficient sunlight, the growth  
387 of organisms on the east-facing surface is not as robust as on the west-facing surface. The west-  
388 facing surface receives sunlight in the afternoon when the rock surface temperature is higher,  
389 providing both water and heat conditions that are more favorable for biological growth. This results  
390 in the presence of *Scytonema sp.1*, a cyanobacterium that prefers looser substrates, and more mosses,  
391 leading to more severe weathering on the west-facing surface. The north-facing surface, being in  
392 the shade, has slower evaporation rates and is mainly colonized by spherical cyanobacteria, resulting

393 in relatively weaker weathering. The south-facing surface receives more sunlight and weathers faster,  
394 with the carved decorations on the rock surface completely destroyed (Fig. 13a). The matrix is  
395 highly loose, and even large filamentous cyanobacteria like *Nostoc*, which typically prefer to live  
396 in soil rather than on rock surfaces, are present. This indicates that the south-facing marble has  
397 weathered severely, forming a loose, soil-like thick weathering layer. Additionally, *Scytonema* sp.1,  
398 a species that thrives in sunny and dry environments and plays a significant role in bioweathering,  
399 is also present. Mosses are not found on the south-facing side because they prefer shady and moist  
400 environments. The orientation of the building, through differences in sunlight duration and  
401 evaporation rates, creates a unique gradient of microhabitats, which in turn drives the differential  
402 distribution of microbial communities and is accompanied by varying degrees of weathering  
403 depending on the direction.

404 To further understand the environmental differences and weathering conditions of the rock  
405 surfaces at the Hall of Prayer for Good Harvests in the Temple of Heaven, temperature  
406 measurements were taken on a sunny afternoon in April (Fig. 16). The rock surface temperatures  
407 were found to be highest in the southwest and lowest in the northwest. The Hall of Prayer for Good  
408 Harvests was divided into four natural sectors, each centered on a cardinal direction and covering  
409 45° to either side: North (N): 315°-45°, centered on true north, covering from northwest to northeast;  
410 East (E): 45°-135°, centered on true east, covering from northeast to southeast; South (S): 135°-  
411 225°, centered on true south, covering from southeast to southwest; West (W): 225°-315°, centered  
412 on true west, covering from southwest to northwest. The weathering degree of 100 Cloud Chi Heads  
413 on the third layer was statistically analyzed in each sector. The results showed that 40% of the south-  
414 facing Cloud Chi Heads decorations were completely weathered, indicating the most severe  
415 weathering. The weathering degrees for the west, east, and north sectors decreased in that order.  
416 This pattern is consistent with the distribution of biological organisms on the rock surfaces, as shown  
417 in Table 1. The analysis of the weathering degree of 100 Cloud Chi Heads on the third layer showed  
418 that 40% of the south-facing Cloud Chi Heads decorations were completely weathered, indicating  
419 the most severe weathering. The weathering degrees for the west, east, and north directions  
420 decreased in that order. This pattern is consistent with the differences in weathering in different  
421 directions revealed by the distribution of biological organisms on the rock surfaces (Table 1).



422

423 Fig. 16 Rock surface temperatures and weathering conditions of the Cloud Chi Heads on the third layer of the  
424 Hall of Prayer for Good Harvests at the Temple of Heaven in Beijing, China, on a sunny afternoon in April.  
425 a: Cloud Chi Heads with complete decorative structures.  
426 b: Cloud Chi Heads with partially weathered decorative structures.  
427 c: Cloud Chi Heads with completely weathered decorative structures.  
428 d: A simplified top view of the Hall of Prayer for Good Harvests shows that its base is divided into three tiers, with 100 Chi Heads  
429 arranged along the edge of each tier. The Chi Heads exhibit different degrees of weathering. This article has documented the weathering of  
430 the outermost layer of Cloud Chi Heads: Red indicates that the decorative structure of Cloud Chi Heads is completely weathered; Yellow  
431 indicates that the decorative structure of Cloud Chi Heads is partially weathered; Green indicates that the decorative structure of Cloud Chi  
432 Heads is still intact.

433 e: Statistical count of the number of Cloud Chi Heads with three different weathering degrees in four directions.

434 f: Calculation of the proportion of the three different weathering degrees of Cloud Chi Heads in different directions, revealing that the

435 weathering intensity of the Chi Heads is highest in the south, followed by the west, east, and north.

436 **Table 1**

437 Environmental characteristics and dominant species of marble surface of the Hall of Prayer for Good  
 438 Harvests at the Temple of Heaven in Beijing, China.

439

Marble Surface Orientation	Sunlight	Moisture	Environmental Characteristics	Dominant Species	Weathering degree
North-facing	None	Slow evaporation	Cold and humid	Spherical cyanobacteria	
East-facing	Half day	Rapid evaporation in the morning	Warm and humid	Small filamentous cyanobacteria,	Weak
				Spherical cyanobacteria	
West-facing	Half day	Rapid evaporation in the afternoon	Hot and humid	Small filamentous cyanobacteria,	Strong
				Mosses	
South-facing	Full day	Rapid evaporation during the day	Hot and dry	Small filamentous cyanobacteria,	
				Large filamentous cyanobacteria	

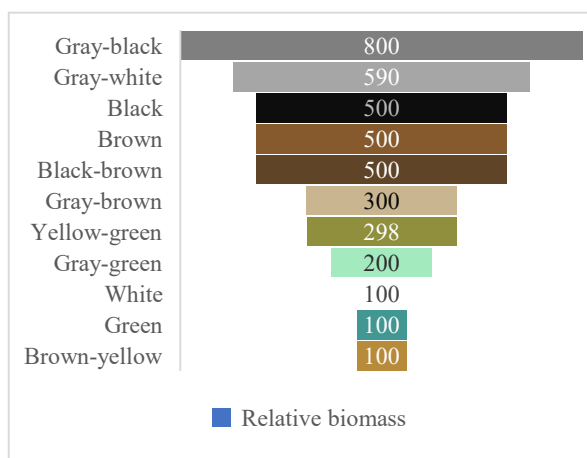
440

### 441 **3.3 Relative Biomass of Different Colored Biological Communities on Rock Surfaces in the Study**

#### 442 **Area**

443 The colors displayed by organisms on rock surfaces differ from those observed under a  
 444 microscope. In this paper, the former is referred to as the "visual color," while the latter is called the  
 445 "microscopic color." The visual color is the community color presented when different populations  
 446 aggregate together, whereas the microscopic color is the color of different species observed under  
 447 magnification through a microscope. Often, communities of cyanobacteria with different  
 448 microscopic colors appear mostly black or gray-black of visual color.

449 The visual colors of biological communities on rock surfaces in the study area can be  
 450 categorized into gray-black, gray-white, black, brown, black-brown, gray-brown, yellow-green,  
 451 gray-green, white, green, and brown-yellow. Their relative biomass is shown (Fig. 17) . The most  
 452 common color is gray-black, followed by gray-white, black, brown, and black-brown. These are  
 453 also typical colors exhibited by aerophytic cyanobacteria in the field, sometimes referred to as "ink  
 454 bands." For example, the Nine Horses Fresco Hill (Jiuma Huashan) in the Guilin landscape of China  
 455 is formed due to aerophytic cyanobacteria growing on the rocks, creating black ink-like bands.



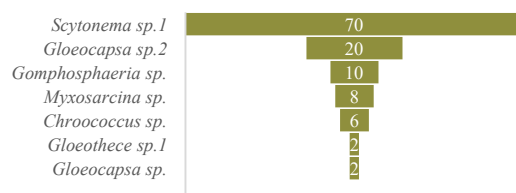
456  
 457 **Fig. 17** Relative biomass of biomes with different colors on the marble surface of the Hall of Prayer for Good  
 458 Harvests at the Temple of Heaven in Beijing, China.

459  
 460 3.4 Relative biomass of communities' composition in different colored biological communities on  
 461 rock surfaces in the study area

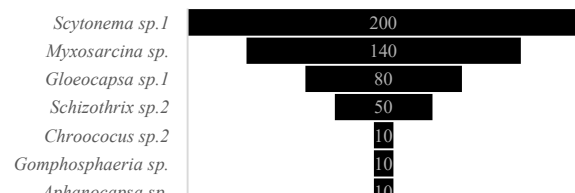
462 The relative biomass of different visual color biotic communities on the rock surface in the  
 463 study area is shown (Fig. 18). An analysis of the main population compositions of these biological  
 464 communities is presented (Fig. 19). The colors of biological communities on rock surfaces in the  
 465 study area are primarily composed of black, brown, gray, green, and yellow, as well as combinations  
 466 of these colors (gray-black, gray-white, black-brown, gray-brown, yellow-green, gray-green, and  
 467 brown-yellow). The correlation between color combinations and population composition is not very  
 468 apparent, which also indicates that determining microscopic color (population composition) through  
 469 visual color is a complex and difficult task. Nevertheless, some patterns can be observed: Species  
 470 like *Scytonema* sp.1, *Myxosarcina* sp., *Asterocapsa* sp., *Gomphosphaeria* sp., and *Gloeocapsa* sp.2  
 471 tend to make the community color darker, presenting as black, brown, gray, or combinations of these;

472 The parts that have a visual color of white are minerals, not biological organisms, under microscopic  
 473 observation; the areas with a visual color of green (mainly referring to the characteristic blue-green  
 474 of cyanobacteria) are mineral particles and *Chroococcus* sp.1; the areas with a visual color of  
 475 yellow-green are mainly mosses; the areas with a visual color of brown-yellow are mainly *Nostoc*  
 476 sp. etc.

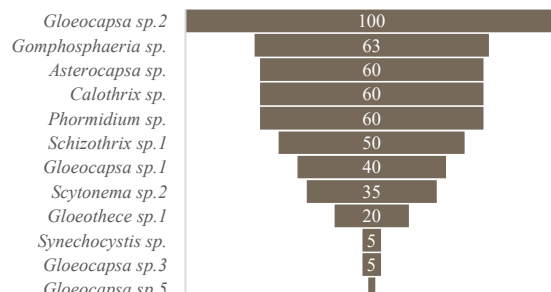
477



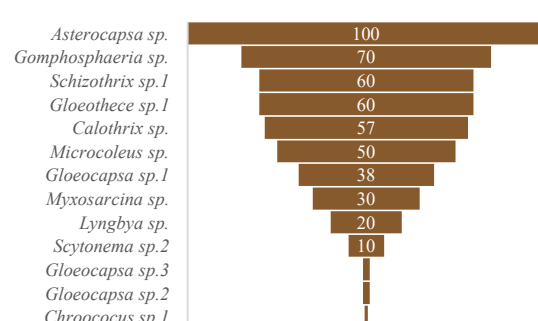
■ Yellow-green biome relative biomass



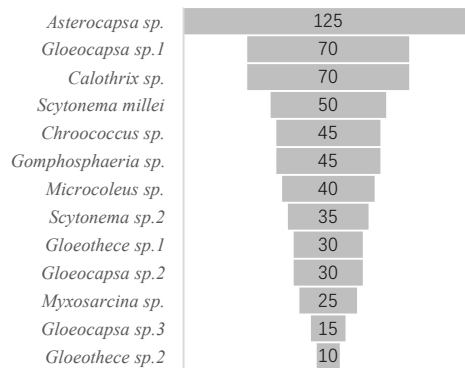
■ Black biome relative biomass



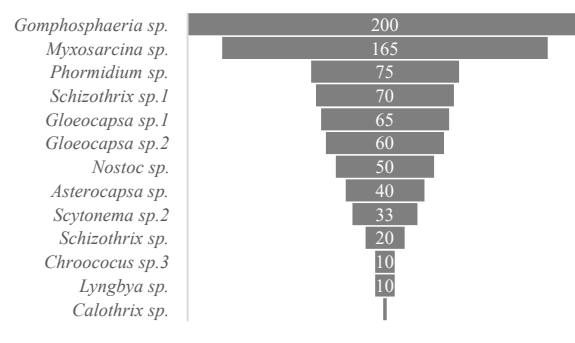
■ Gray-brown biome relative biomass



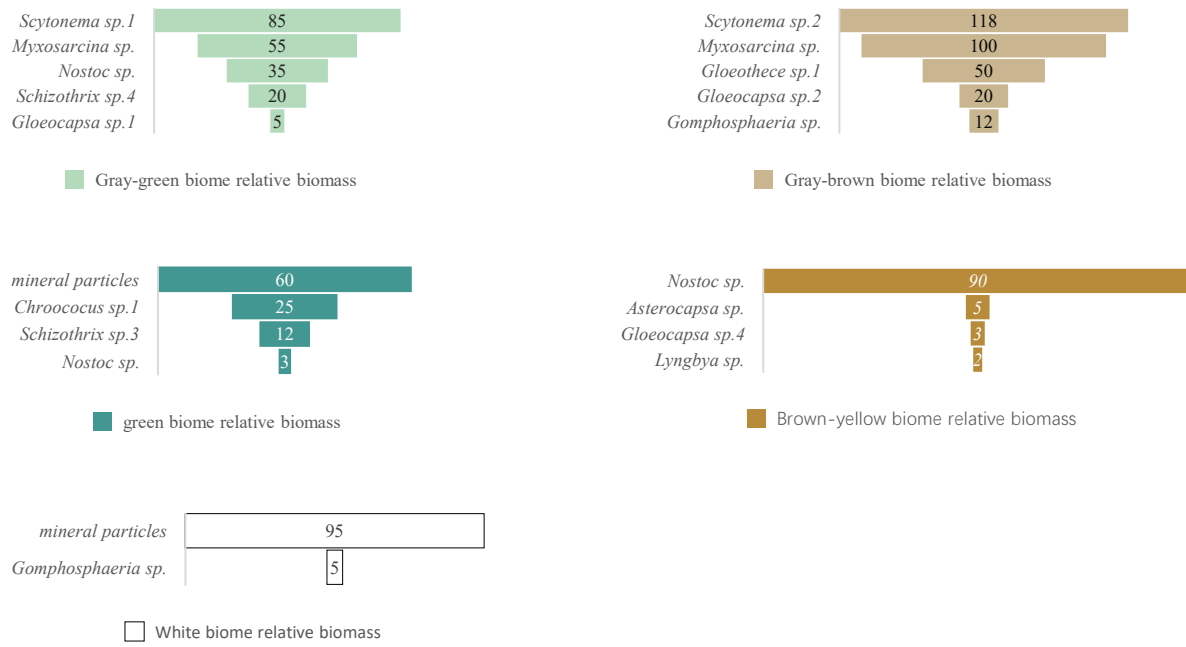
■ Brown biome relative biomass



■ Gray-white biome relative biomass



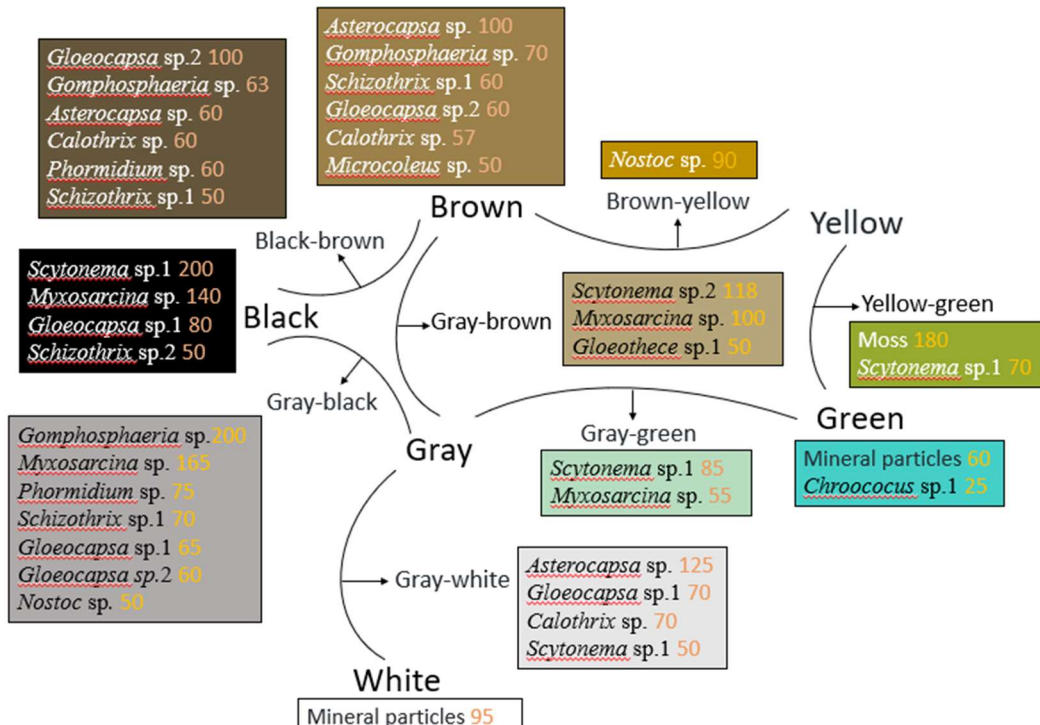
■ Gray-black biome relative biomass



478 **Fig. 18.** Relative biomass of community composition of different colors on marble surface of the Hall of Prayer for

479 Good Harvests at the Temple of Heaven, China.

480



481

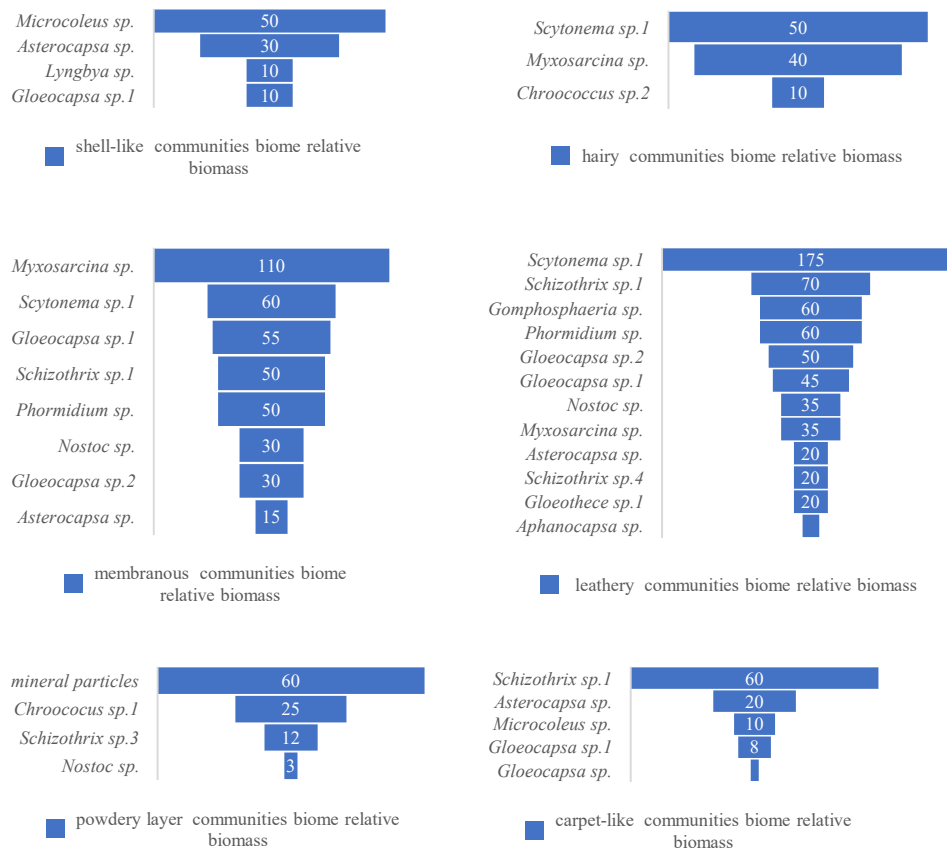
482 **Fig. 19.** Analysis of main population composition of different color biomes on marble surface of the Hall of Prayer

483 for Good Harvests at the Temple of Heaven in Beijing, China.

484

485 3.5 Relative biomass of communities composition in different morphological biological  
 486 communities on rock surfaces in the study area

487 The biological communities on rock surfaces in the study area exhibit different morphologies,  
 488 including membranous, hairy, carpet-like, leathery, shell-like, and powdery layers. Their relative  
 489 biomass of population composition is shown (Fig. 20). A diagrammatic explanation of the formation  
 490 of these community morphologies is presented (Fig. 21).



491 **Fig. 20.** Relative biomass of different forms of community on marble surface of the Hall of Prayer for Good  
 492 Harvests at the Temple of Heaven in Beijing, China.  
 493

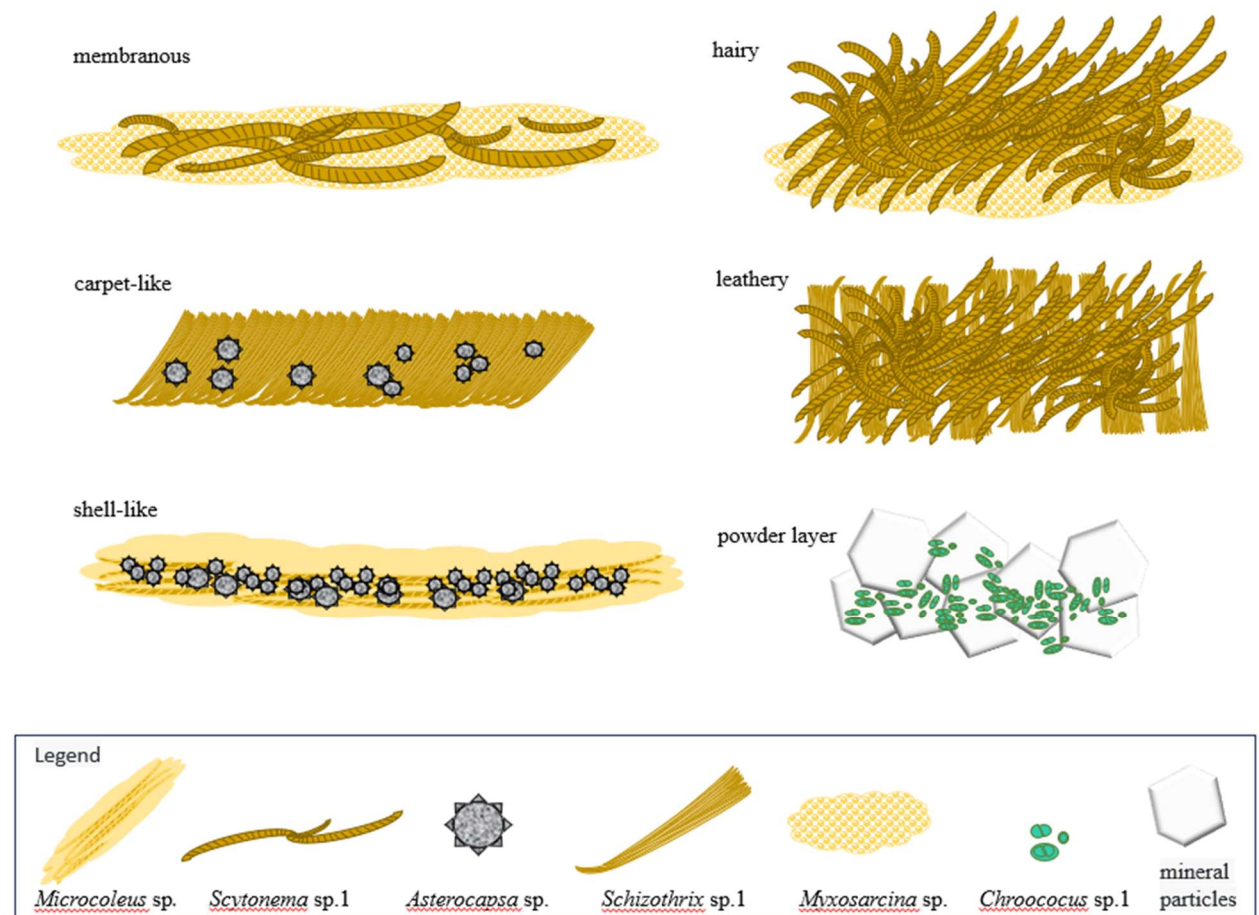


**Fig. 21** Morphological genesis diagram of different communities on marble surface of the Hall of Prayer for Good

Harvests at the Temple of Heaven in Beijing, China.

The dominant species in the membranous biological communities are mainly *Myxosarcina* sp. and *Scytonema* sp.1. The former accounts for a relative biomass of 110, while the latter accounts for 60 (Fig. 17) . *Myxosarcina* sp. is spherical cyanobacteria (Fig.4a). It has thick individual sheaths, forming a dense colonial mucilage. *Scytonema* sp.1 grows interspersed within, forming a membrane-like community (Fig.21). When the relative biomass of *Scytonema* sp.1 in the community exceeds that of *Myxosarcina* sp., it forms a hairy community (Fig.21). The dominant species in the carpet-like communities are mainly *Schizothrix* sp.1 and *Asterocapsa* sp. The former accounts for a relative biomass of 60, while the latter accounts for 20 (Fig.20). *Schizothrix* sp.1 grows densely together, forming a carpet-like structure (Fig. 21). The dominant species in the leathery biological communities are mainly *Scytonema* sp.1 and *Schizothrix* sp.1. The former accounts for a relative biomass of 175, while the latter accounts for 70 (Fig. 20). *Scytonema* sp.1

509 intertwines, with *Schizothrix* sp.1 interspersed within (Fig. 21). The dominant species in the shell-  
510 like biological communities are mainly *Microcoleus* sp. and *Asterocapsa* sp. The former accounts  
511 for a relative biomass of 50, while the latter accounts for 30 (Fig.20). *Microcoleus* sp. has well-  
512 developed sheaths, with multiple algal filaments inside each sheath. The sheaths of multiple  
513 *Microcoleus* sp. aggregate to form a mucilaginous layer, with *Asterocapsa* sp.1 dispersed within.  
514 When the mucilaginous layer dries, it cracks into numerous small pieces. The edges of each piece  
515 detach from the rock surface and curl up, forming a shell-like structure (Fig. 21 and Fig. 22) . The  
516 powder layer is a severely weathered surface (Fig. 13d). Under microscopic observation, it mainly  
517 consists of mineral particles and *Chroococcus* sp.1, with the former accounting for 60 and the latter  
518 for 20 of the relative quantity (Fig. 20). *Chroococcus* sp.1 is distributed on the surface and in the  
519 crevices of mineral particles (Fig. 14a and b). The color of the community appears as a mixture of  
520 the green color of *Chroococcus* sp.1 (or the blue-green color characteristic of cyanobacteria) and the  
521 white color of mineral particles.

522

### 523 3.6 Bioweoathering on Rock Surfaces in the Study Area

524 The growth distribution of aerophytic organisms on rock surfaces in the study area is closely  
525 related to the surface smoothness and texture of marble (Table 2). If the marble surface is uneven or  
526 has a non-uniform texture, the aerophytic organisms' communities will be distributed in a spotted  
527 pattern (Fig. 22a). Dissolution forms solution pits and cavities (Fig. 22b), which further expand into  
528 solution basins (Fig. 22c, d). If the marble surface has linear textures or non-uniform texture with  
529 joint stripes, the aerophytic organisms' communities will be distributed in a linear pattern (Fig. 22e).  
530 Dissolution forms solution marks and grooves (Fig.22f), which further expand into solution  
531 channels (Fig. 22g). If the marble surface is smooth and has a uniform texture, the aerophytic  
532 organisms' communities will be distributed in a planar pattern (Fig. 22h). Dissolution forms a  
533 weathering layer or spalling layer (Fig. 22i).

534

### 535 **Table 2**

536 Characteristics of the Marble Surface of the Hall of Prayer for Good Harvests in the Temple of  
537 Heaven, Beijing, China, and the Process of Biological Erosion on Its Surface.

Marble Characteristics	Biological Community	Resulting Dissolution	Development
	Distribution	Forms	Process
Uneven surface or non-uniform texture	Spotted distribution	Solution pits, cavities, and basins	
Surface with linear textures or non-uniform texture with joint stripes	Linear distribution	Solution marks, grooves, and channels	
Smooth surface with uniform texture	Areal distribution	Weathering layer, spalling layer	

538

539

540

541



a. biological community point distribution



b. Solution pores and solution cavities



c. Sinkhole



542 **Fig. 22** Bioweathering forms on the marble surface of the Hall of Prayer for Good Harvests in the Temple of  
 543 Heaven, Beijing, China.

544

545

546 The spotted distribution of biological communities gradually expands into linear distribution,  
 547 and then into areal distribution. Solution pits, basins, and cavities also further enlarge their  
 548 dissolution forms, developing into solution marks, grooves, and channels. For example, in the study

549 area, the weathering process of white marble “Cloud Chi Head” begins with the accumulation and  
550 growth of organisms in the low-lying areas of the cloud patterns (Figures 23a, b).. These areas retain  
551 more moisture, so they are the first to undergo bioweathering, forming deeper solution cavities and  
552 channels. The communities then gradually spread to the surrounding areas, developing into linear  
553 distributions, and then areal distributions, leading to flaking of the rock surface (Fig. 23c). This  
554 partially destroys the pattern structure, further expanding the area and depth of dissolution, forming  
555 a loose powder layer (Fig. 13a, d; Fig. 14a, b; Fig. 16b, c; Fig. 23d, e).

556



a. The organisms gather and  
grow in the low-lying areas of  
the Cloud Chi Head  
ornamentation.

b. The organisms gather and grow  
in the low-lying areas of the Cloud  
Chi Head ornamentation.

c. The surface of the Cloud Chi Head  
is flaking off in patches.



d. The Cloud Chi Heads have even weathered away  
completely.



e. A loose, powdery layer has formed on the surface  
of the Cloud Chi Heads, with a large amount of  
cyanobacteria growing inside.

557

**Fig. 23.** Bioweathering process of the Cloud Chi Head on the Hall of Prayer for Good Harvests in the Temple of

558 Heaven, Beijing, China.

559

560 **4 Discussion**

561 (1) This study focuses on the cyanobacterial and bryophyte communities that can be observed  
562 using biological microscopy. The current scope of the research has not yet covered other microbial  
563 groups. To determine whether other bacterial groups exist on the surface of stone cultural relics and  
564 to understand their ecological functions, further systematic verification through subsequent studies  
565 is still needed. At the methodological level for the classification and identification of cyanobacteria,  
566 traditional morphological identification, although it may lead to taxonomic deviations at the genus  
567 and species levels, molecular biology methods also face technical bottlenecks. For special samples  
568 like biofilms on stone cultural relics, molecular testing typically requires microbial samples with a  
569 high purity of more than 0.2 grams. However, in actual sampling, due to restrictions on cultural relic  
570 protection, sometimes only trace amounts of less than 0.01 grams can be obtained. While such low  
571 sample quantities are sufficient for morphological identification under a biological microscope, they  
572 pose significant challenges for molecular biology methods. Low DNA extraction efficiency and  
573 significant amplification bias from such small samples can result in decreased taxonomic resolution.  
574 Furthermore, there has been long-standing controversy in the taxonomy of cyanobacteria. The  
575 conflict between traditional morphological classification and molecular systematics has led to a  
576 dynamic revision of the taxonomic framework. This instability makes it difficult to match taxonomic  
577 information when annotating environmental samples using 16S rRNA gene sequence databases  
578 (Lefler, et al., 2023). Future research should aim to construct a multidimensional identification  
579 system, integrating microscopic observation, culturomics, and metagenomics, to gradually establish  
580 classification standards and databases suitable for the study of microorganisms in cultural heritage.  
581 This will be an important direction for the development of methodologies in this field.

582 (2) The differential weathering characteristics of the Cloud Chi Heads on the Hall of Prayer for  
583 Good Harvests, as well as the directional differences in the spatial distribution of organisms on the  
584 rock surface, show significant consistency. This correspondence confirms the scientific validity of  
585 the visual analysis method based on the relative volume and the relative volume percentage  
586 determined by microscopic observation. This method, through the analysis of micro-scale biotic  
587 community features, can effectively reflect the differences in weathering processes in the macro-

588 environment, providing an important reference for establishing the correlation between micro-  
589 observation indicators and macro-environmental factors.

590 (3) The bioweathering process of the marble at the Hall of Prayer for Good Harvests in the  
591 Temple of Heaven is controlled by both macro-hydrological dynamics and micro-surface  
592 topography: On a macro scale, in areas with low flow during heavy rain (raised areas), water quickly  
593 drains away, resulting in sparse biofilms and weak bioweathering. In high-flow areas during heavy  
594 rain (water-collecting grooves), the extended water retention time leads to the formation of "ink  
595 bands" rich in cyanobacteria, resulting in strong bioweathering. On a micro scale, the micro-  
596 topographic features of the rock determine the colonization patterns of organisms by regulating local  
597 hydrological conditions—irregular rough surfaces induce point-like biological aggregation due to  
598 discrete water films, leading to the development of solution pores and pits; linear decorations or  
599 joint surfaces promote linear biological expansion due to directional water storage, forming solution  
600 marks and grooves; smooth and dense surfaces support planar biological growth due to uniform  
601 water film coverage, ultimately leading to the overall peeling of the weathered layer. This coupled  
602 mechanism reveals that, in addition to the different sunlight exposure on the rock surface caused by  
603 orientation, the synergistic regulation of spatiotemporal water distribution and rock surface  
604 characteristics is also an important reason for the different distribution of biological communities  
605 on stone cultural relics. Some studies also suggest that the type of stone, its position on the building,  
606 and the surface roughness of the stone greatly influence biological growth (Korkanç and Savran,  
607 2015). Some organisms (such as cyanobacteria and lichens) also bore into the marble, forming a  
608 hard, black, porous layer (Golubić, et al., 2015). The biological black crust on marble is often  
609 attributed to physical and inorganic chemical causes such as dust, which needs to be taken seriously.

610 (4) The connections and issues between different research levels, methods, and results in this  
611 paper.

612 Connections and issues between different research levels, methods, and results in this paper.  
613 This paper studies the aerophytic organisms on rock surfaces in the research area in terms of  
614 biological community population composition, community color and morphology, and community  
615 distribution characteristics (Table 3). The spotted, linear, and planar distributions of biological  
616 communities on rock surfaces in the study area are composed of many microcommunities. These  
617 microcommunities exhibit different morphologies, including membranous, hairy, carpet-like,

618 leathery, shell-like, and powder layers. Spotted, linear, and areal distributions of biological  
619 communities may be composed of one type of microcommunity or multiple types.  
620 Microcommunities are further composed of multiple populations, and a population consists of  
621 multiple individual organisms of the same species.

622 Community distribution characteristics are observed with the naked eye, without  
623 magnification. Community color and shape are observed through stereomicroscopes and the naked  
624 eye, magnifying objects 8-56 times (or no magnification if observed with the naked eye). Biological  
625 community population composition is identified through biological microscope observation,  
626 magnifying objects 40-1000 times. This represents three stages of research with increasing  
627 magnification of the research object: 1) Distribution area; 2) Community; 3) Population. Research  
628 at each stage is relatively easy to conduct, but the connections between stages are challenging and  
629 represent a key focus of this paper. For example, to accurately correlate different colored and shaped  
630 communities with their precise population compositions (i.e., connecting the community stage with  
631 the population stage) requires statistical analysis of numerous specimens to improve accuracy.  
632 Additionally, for outdoor observations of communities, which involve the transition between the  
633 distribution area stage and the community stage, the primary method is still visual observation with  
634 the naked eye. Only a small number of observations are conducted using stereomicroscopes because  
635 detailed stereomicroscopic observations that require photography must be done indoors. Sampling  
636 of cultural relics in scenic areas is extremely limited and must be carried out without damaging the  
637 relics. To address this issue, one approach is to enhance the performance of observation equipment  
638 to allow for in situ biological community observations outdoors without sampling, or to perform  
639 minimal sampling.

640 **Table 3**

641 Analysis of Research Levels in the Study on aerophytic organisms on marble of the Hall of Prayer for Good  
642 Harvests in the Temple of Heaven, Beijing, China.

Research Level	Distribution Area	Community	Population
Observation Method	Naked eye	Stereomicroscope, naked eye	Biological microscope
Magnification	0	8-56, 0	40-1000

---

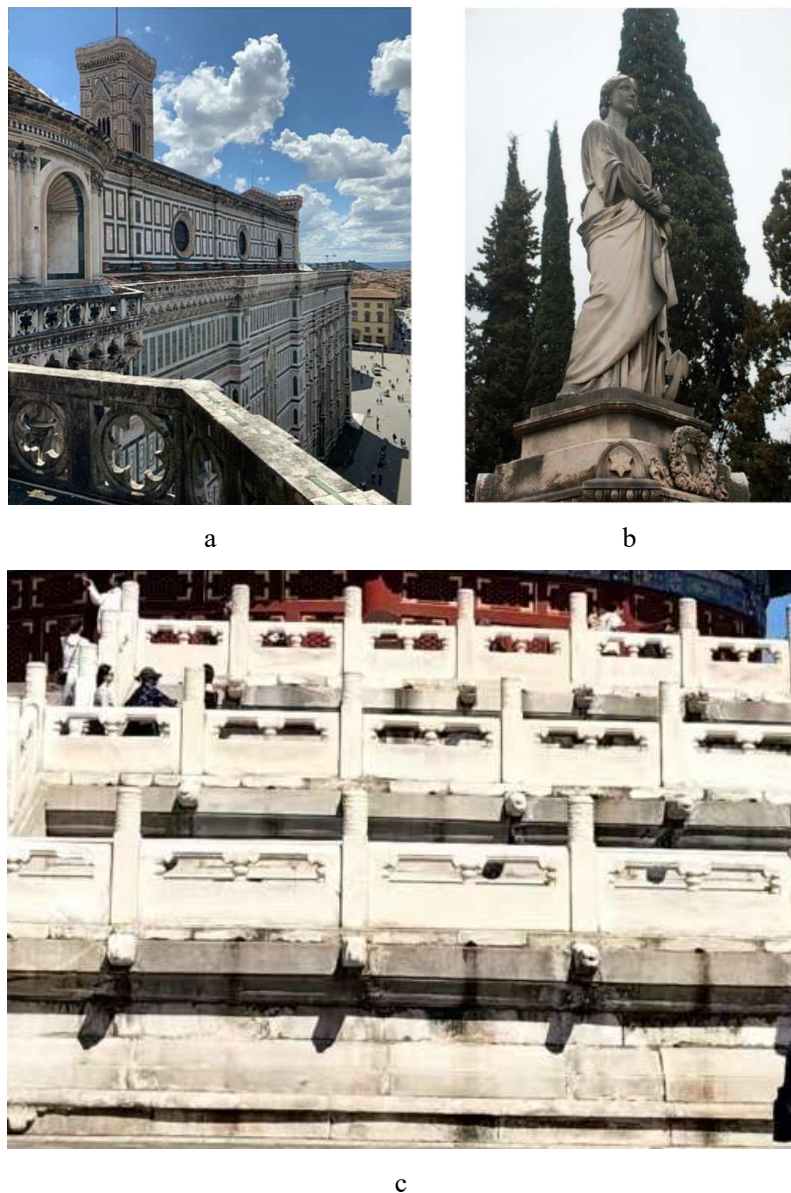
		11 colors:		
		gray-black, gray-white,		
		black, brown, black-brown,	30 genera and	
		gray-brown, yellow-green,	species :	
	Classification	3 distribution characteristics (point, linear, and areal distribution)	gray-green, white, green, brown-yellow	
			<i>Myxosarcina</i> sp., <i>Gomphosphaeria</i> sp., <i>Asterocapsa</i> sp.	
		6 morphologies:	membranous, hairy, carpet- like, leathery, shell-like, and powder layer	
			and so on (Fig.5)	
	Composition	Composed of multiple communities	Composed of multiple populations	Composed of multiple individuals of a single species

---

643

644 (5) In this study, the weathering intensity of the Hall of Prayer for Good Harvests in the Temple of  
 645 Heaven is found to be south-facing > west-facing > east-facing > north-facing. Additionally, the  
 646 metabolic activity of the southeastern microbial community on the marble of Florence Cathedral is  
 647 higher than that of the northwestern community (Checcucci, et al., 2022). This indicates that the  
 648 weathering of stone cultural relics exhibits directional differences, and these directional differences  
 649 vary in different climate zones. When studying the microenvironment of rock surfaces, temperature  
 650 is relatively easy to measure, but humidity is difficult to measure accurately due to the significant  
 651 influence of wind disturbances, which can lead to measurement failures. Therefore, more effective  
 652 methods are needed to address this issue. Another comparison can be made between the marble  
 653 relics of the Cathedral of Santa Maria del Fiore in Florence, Italy, and the Speranza statue (the  
 654 Cathedral of Santa Maria del Fiore was completed in 1887 and is 135 years old; the Speranza statue  
 655 was built in 1863 and is 158 years old). The growth of black biofilm on these structures is  
 656 significantly more extensive and faster than that on the Hall of Prayer for Good Harvests at the  
 657 Temple of Heaven in Beijing (built in 1420 and 605 years old). The primary reason for this  
 658 difference is the climate. Florence has a Mediterranean climate with high rainfall (about 850 mm)  
 659 (Venturi et al., 2020), while Beijing has a temperate monsoon climate with low annual rainfall

660 (During the period from 2009 to 2024, the multi-year average annual total rainfall was 610 mm,  
661 according to data from the National Meteorological Science Data Center Website.). Therefore, water  
662 is the primary factor determining the growth rate and distribution area of the black biofilm on marble.  
663 Additionally, the different physical properties of marble in the two locations should also be  
664 considered.



665 Fig. 24: Comparison of Black Biofilm Growth on Marble Relics in Florence and Beijing

666 a. Cathedral of Santa Maria del Fiore in Florence (façade completed in 1887, 138 years old, using white, green, and pink marble), with a  
667 large area covered by black biofilm (Santo, 2023);  
668 b. Speranza statue in Florence (built in 1863, 158 years old, using white marble), with a large area covered by black biofilm (Mascalchi,  
669 2018);

670 c. The Hall of Prayer for Good Harvests at the Temple of Heaven in Beijing (built in 1420, 605 years old, using white and bluish-white  
671 marble), with a small area covered by black biofilm, mainly distributed in areas with high runoff from sudden rain.

672 (6) The species in the study area, such as *Scytonema* sp.2, are also common aerophytic cyanobacteria  
673 found on limestone surfaces (Tian, et al., 2002; Tian, et al., 2003; Tian, et al., 2004). They prefer  
674 calcareous environments, are drought-resistant, grow slowly, and have extremely strong vitality.  
675 The mechanism of dissolve rocks primarily involves the biological need to obtain inorganic  
676 nutrients such as calcium and magnesium ions from the rock. Aerophytic organisms can secrete  
677 organic acids, which release calcium and magnesium ions from the rock, providing the inorganic  
678 nutrients necessary for their growth and development. Through this acid dissolution process,  
679 aerophytic organisms can "eat away" at the rock, forming small hemispherical dissolution pits. This  
680 process damages the surface structure of the rock, leading to the formation of an underlying  
681 weathering layer (Tian, et al., 2004). In addition, various forms of cyanobacterial communities in  
682 extremely arid environments, such as on rocks, develop thicker exopolysaccharide (EPS) sheaths to  
683 retain intracellular water. The EPS sheath undergoes contraction and expansion in response to  
684 changes in weather conditions, accelerating the disintegration of rock particles on the surface of  
685 rocks. This process is very similar to microbial weathering in the Atacama Desert (Jung, et al., 2020).  
686 Both processes involve the swelling of the EPS due to water absorption, leading to the deformation  
687 of the biofilm and the detachment of the rock surface at the community scale. This results in the  
688 expansion of patchy weathering into a more extensive weathering layer (such as the Atacama  
689 terrestrial protopellic or the powdery layer at the Temple of Heaven) at the landscape scale. The  
690 mechanism involves the tensile stress generated by the swelling of the EPS exceeding the local  
691 tensile strength of the rock, initiating cracks (such as grain boundary cracking in the Atacama and  
692 mineral particle detachment at the Temple of Heaven). These cracks provide pathways for chemical  
693 and biological erosion, leading to an expanded pore/crack network, increased water retention time,  
694 enhanced biological activity, and further swelling, creating a self-reinforcing weathering loop. It is  
695 clear that the swelling effect plays a crucial role as a "physical engine" in microbial bioweathering.  
696 Future research should focus on cross-scale mechanical modeling: scaling up the swelling force of  
697 microbial EPS (at the nN level) to the point of rock fracture (at the MPa level) to reveal the  
698 mechanisms of scale transition; quantifying the impact of changes in fog/rain patterns under global  
699 warming on the frequency of biological swelling, to warn of accelerated weathering risks; and

700 recognizing that swelling not only acts as a "trigger" for rock destruction but also serves as a key  
701 link between biological activity and surface processes. Its universality across different environments  
702 provides a new perspective for understanding the evolution of the Earth's critical zone.

703

704 **5 Conclusion**

705 (1) The most dominant species on marble surfaces in the study area is *Myxosarcina* sp., followed  
706 by *Gomphosphaeria* sp., *Asterocapsa* sp.1, *Gloeocapsa* sp.1, and *Scytonema* sp.1. These  
707 aerobic cyanobacteria prefer calcareous environments, are drought-tolerant, slow-growing, and  
708 extremely resilient.

709 (2) The biological population composition on marble surfaces facing different directions of the Hall  
710 of Prayer for Good Harvests in the Temple of Heaven varies due to differences in sunlight  
711 exposure. The east-facing side, warm and humid, mainly hosts small filamentous and spherical  
712 cyanobacteria such as *Scytonema* sp.2 and *Gomphosphaeria* sp. The west-facing side, hot and  
713 humid, primarily features *Scytonema* sp.1 and mosses, with *Scytonema* sp.1 being small  
714 filamentous cyanobacteria. The north-facing side, cold and humid, mainly supports spherical  
715 cyanobacteria like *Myxosarcina* sp. and *Gomphosphaeria* sp. The south-facing side, hot and dry,  
716 primarily hosts small or large filamentous cyanobacteria such as *Scytonema* sp.1 and *Nostoc*  
717 sp.. The observed weathering intensity in different directions is: south > west > east > north,  
718 which is entirely consistent with the varying degrees of weathering reflected by the Cloud Chi  
719 Heads in each direction. This indicates that the visual analysis method based on the relative  
720 volume and relative volume percentage of species, as determined by microscopic observation  
721 and statistical analysis, is scientifically valid.

722 (3) Rock surface biological communities in the study area display various colors, with gray-black  
723 being the most common, followed by gray-white, black, brown, and brown-black. Gray-black  
724 communities are mainly composed of *Myxosarcina* sp. and *Gomphosphaeria* sp.

725 (4) Rock surface biological communities in the study area exhibit different morphologies, including  
726 membranous, hairy, carpet-like, leathery, shell-like, and powder layers. Different morphologies  
727 correspond to different population compositions.

728 (5) In addition to sunlight exposure, the growth of aerial organism on the rock surfaces in the study  
729 area is also controlled by macro-hydrological dynamics and micro-surface topography. On a

730 macro scale, in areas with low flow during heavy rain, the biofilm is sparse, and the  
731 bioweathering effect is weak. In areas with high-flow areas during heavy rain, "ink bands" rich  
732 in cyanobacteria form, leading to strong bioweathering. On a micro scale, the microtopographic  
733 features of the rock regulate local hydrological conditions, determining the colonization  
734 patterns of the organisms: On uneven or heterogeneous marble surfaces, aerial organism  
735 communities are distributed in patches, leading to the formation of solution pores, cavities, and  
736 pits; On marble surfaces with linear patterns or heterogeneous textures with joint lines, aerial  
737 organism communities are distributed in linear patterns, leading to the formation of solution  
738 marks, grooves, and channels. On flat and homogeneous marble surfaces, aerial organism  
739 communities are distributed in a planar pattern, leading to the formation of weathering layers  
740 or spalling layers. The thicker exopolysaccharide (EPS) sheath of aerophytic cyanobacteria can  
741 undergo contraction and expansion, thereby accelerating the disintegration of rock particles on  
742 the surface of rocks. Preventing or reducing the growth of aerial organism is key to slowing  
743 down the bioweathering process of the marble at the Hall of Prayer for Good Harvests in the  
744 Temple of Heaven.

745

#### 746 **Author contributions**

747 YT completed all the work on the paper, including sampling, photography, experimental data  
748 analysis, charting, drawing, and writing the paper, among other tasks.

749

#### 750 **Competing interests**

751 The author has declared that there are no competing interests.

752

#### 753 **Acknowledgement**

754 This study was supported by National Science Foundation of China (Grant No. 40872197) and the  
755 Development Fund of China University of Geosciences (Beijing) (Grant No. F02114).

756

#### 757 **References**

758 Beijing Institute of Ancient Architecture.: Research and Application of Stone Structure Protection  
759 in Ancient Buildings in Beijing. Beijing: China Literature and History Press. 1-330, 2018.

760 C. Gaylarde, C.: Influence of Environment on Microbial Colonization of Historic Stone Buildings  
761 with Emphasis on Cyanobacteria. Heritage. 3. 1469-1482.  
762 <https://doi.org/10.3390/heritage3040081>, 2020

763 Checcucci, A, Borruso, L, Petrocchi, D, Perito, B.: Diversity and metabolic profile of the microbial  
764 communities inhabiting the darkened white marble of Florence Cathedral. International  
765 Biodeterioration & Biodegradation, 171- . <https://doi.org/10.1016/j.ibiod.2022.105420>, 2022.

766 Danin, A., Caneva, G.: Deterioration of limestone walls in Jerusalem and marble monuments in  
767 Rome caused by cyanobacteria and cyanophilous lichens. International Biodeterioration,  
768 26(6): 397-417, [https://doi.org/10.1016/0265-3036\(90\)90004-Q](https://doi.org/10.1016/0265-3036(90)90004-Q), 1990

769 Desikachary, T. V.: Cyanophyta. Indian Council of Agricultural Research. New Delhi.1~669.  
770 <https://doi.org/10.1086/403350>, 1959

771 Fott, B. (Translated by Luo,d.): Phycology. Shanghai: Shanghai Science and Technology Press. 11-  
772 396, 1980.

773 Geitler, L.: Cyanophyceae. In L.Rabenhorst'S Kryptogamen-Flora, Band 14. Leipzig, Germany:  
774 Akademische Verlagsgesellschaft m.b.H..1~1194, 1932.

775 Gioventù, E., Lorenzi, P. F., Villa, F., Sorlini, C., Rizzi, M., Cagnini, A., Griffo, A., Cappitelli, F.:  
776 Comparing the bioremoval of black crusts on colored artistic lithotypes of the Cathedral of  
777 Florence with chemical and laser treatment. International Biodeterioration & Biodegradation,  
778 65(6): 832-839, <https://doi.org/10.1016/j.ibiod.2011.06.002>, 2011

779 Golubić, S, Pietrini, A M, Ricci, S.: Euendolithic activity of the cyanobacterium Chroococcus  
780 lithophilus Erc. In biodeterioration of the Pyramid of Caius Cestius, Rome, Italy.  
781 International Biodeterioration & Biodegradation, 100: 7-16,  
782 <https://doi.org/10.1016/j.ibiod.2015.01.019>, 2015

783 Gorbushina, A. Lyalikova, N. Vlasov, D.Y. Khizhnyak, T.: Microbial communities on the  
784 monuments of Moscow and St. Petersburg: biodiversity and trophic relations. Microbiology,  
785 71, 350-356, <https://doi.org/10.1023/A:1015823232025>, 2002

786 Guiamet, P., Crespo, M., Lavin, P., Ponce, B., Gaylarde, C., Saravia, S. G. D.: Biodeterioration of  
787 funeral sculptures in La Recoleta Cemetery, Buenos Aires, Argentina: Pre- and post-  
788 intervention studies. Colloids and Surfaces B: Biointerfaces, 101: 337-342,  
789 <https://doi.org/10.1016/j.colsurfb.2012.06.025>, 2013.

790 Guillitte, O., Dreesen, R: Laboratory chamber studies and petrographical analysis as bioreceptivity  
791 assessment tools of building materials, *Science of The Total Environment*, Volume 167,  
792 Issues 1–3, 365-374, [https://doi.org/10.1016/0048-9697\(95\)04596-S](https://doi.org/10.1016/0048-9697(95)04596-S), 1995

793 He, H.: Study on the Weathering of Marble Jinshi Steles in Beijing Confucius Temple. *Capital*  
794 *Museum Forum*, (35): 226-231, 2021.

795 Hu, H., Wei, Y. (Editors): *Systematics, Classification, and Ecology of Freshwater Algae in China*.  
796 Beijing: Science Press. 23-203, 2006.

797 Isola, D., Zucconi, L., Onofri, S., Caneva, G., Selbmann, L.: Extremotolerant rock inhabiting black  
798 fungi from Italian monumental sites. *Fungal Diversity* 76, 75–96.  
799 <https://doi.org/10.1007/s13225-015-0342-9>, 2016

800 Jung, P., Baumann, K., Emrich, D., Springer, A., Felde, V. J. M. N. L., Dultz, S., Baum, C., Frank,  
801 M., Büdel, B., Leinweber, P.: Lichens Bite the Dust – A Bioweathering Scenario in the  
802 Atacama Desert. *iScience*, 23, 101647. <https://doi.org/10.1016/j.isci.2020.101647>, 2020

803 Komarek, J., Anagnostidis, K.: *Cyanoprokaryota 1. Teil: Chroococcales*. Vol. 19(1), In: Ettl H.,  
804 Gaertner G, Heynig, H. and Mollenhauer, D. (eds.), *Suesswasserflora von Mitteleuropa*, Gustav  
805 Fischer, Jena-Stuttgart-Luebeck:Ulm. 1-548. <https://doi.org/10.2216/i0031-8884-38-6-544.1>,  
806 1998.

807 Komarek, J., Anagnostidis, K.: *Cyanoprokaryota 2. Teil: Oscillatoriales*. Vol. 19(2), In: Büdel B.,  
808 Gärtnner G, Krienitz, L. and Schagerl, M. (eds.), *Suesswasserflora von Mitteleuropa*. Heidelberg,  
809 Germany: Springer Spektrum. 1-759, 2005.

810 Komarek, J., Büdel, B., Gärtnner, G. *Süßwasserflora von Mitteleuropa*, Bd. 19/3: *Cyanoprokaryota*:  
811 3. Teil / 3rd part: *Heterocytous Genera*. Springer Spektrum, 2013

812 Korkanç, M, Savran, A.: Impact of the surface roughness of stones used in historical buildings on  
813 biodeterioration. *Construction and Building Materials*, 80: 279-294,  
814 <https://doi.org/10.1016/j.conbuildmat.2015.01.073>, 2015

815 Lefler, F.W., Berthold, D.E., Laughinghouse, H. D.: *Cyanoseq*: A database of cyanobacterial 16S  
816 rRNA gene sequences with curated taxonomy. *J. Phycol.*, 59: 470-480,  
817 <https://doi.org/10.1111/jpy.13335>, 2023.

818 Leo, F., D., Antonelli, F., Pietrini, A., M., Ricci, S., Urzì, C.: Study of the euendolithic activity of  
819 black meristematic fungi isolated from a marble statue in the Quirinale Palace's Gardens in

820 Rome, Italy. *Facies*, 65,18, <https://doi.org/10.1007/s10347-019-0564-5>, 2019

821 Li, J.: Research on mechanical properties evaluation and deterioration mechanism of heritage rock  
822 in different environment. Master's Thesis. Beijing: Beijing University of Civil Engineering  
823 and Architecture. 1-72. <https://link.cnki.net/doi/10.26943/d.cnki.gbjzc.2023.000478>, 2023.

824 Liu, J.: Experimental study of thermal effects on Physical-mechanical properties of Beijing  
825 dolomitic marble. Master's Thesis. Beijing: China University of Geosciences (Beijing). 1-78.  
826 <https://link.cnki.net/doi/10.27493/d.cnki.gzdzy.2020.001911>, 2020.

827 Lombardozzi, V., Castrignanò, T., Antonio, M. D., Municchia, A C, Caneva, G.: An interactive  
828 database for an ecological analysis of stone biopitting. *International Biodeterioration &*  
829 *Biodegradation*, 73: 8-15, <https://doi.org/10.1016/j.ibiod.2012.04.016>, 2012

830 Lü, J., Wei, J.: Contribution of Dashiwo Marble in Fangshan, Beijing to the Foundation of the  
831 Forbidden City and Stone Sutras of Yunju Temple. *Fossil*, (03): 68-73, 2020.

832 Macedo, M F , Miller, A Z, Dionísio, A, Saiz-Jimenez, C: Biodiversity of cyanobacteria and green  
833 algae on monuments in the Mediterranean Basin: An overview. *Microbiology*, 155(Pt 11): 3476-  
834 3490. <https://doi.org/10.1099/mic.0.032508-0>, 2009

835 Marvasti, M., Cavalieri, D., Mastromei, G., Casaccia, A., Perito, B.: Omics technologies for an in-  
836 depth investigation of biodeterioration of cultural heritage. *Int. Biodeterior. Biodegrad.*, 144,  
837 <https://doi.org/104736>, 10.1016/j.ibiod.2019.104736, 2019

838 Marvasti, M., Donnarumma, F., Frandi, A., Mastromei, G., Sterflinger, K., Tiano, P., Perito, B.: Black  
839 microcolonial fungi as deteriogens of two famous marble statues in Florence, Italy,  
840 International Biodeterioration & Biodegradation, Volume 68, 36-44,  
841 <https://doi.org/10.1016/j.ibiod.2011.10.011>, 2012

842 Mascalchi, M., Osticioli, I., Cuzman, O. A., Mugnaini, S., Giampello, M., Siano, S.: Laser removal  
843 of biofilm from Carrara marble using 532 nm: The first validation study, *Measurement*, V.  
844 130, 255-263, <https://doi.org/10.1016/j.measurement.2018.08.012> , 2018

845 Miller, A., Dionísio, A., Macedo, M. F.: Primary bioreceptivity: A comparative study of different  
846 Portuguese lithotypes. *International Biodeterioration & Biodegradation*, 57(2): 136-142.  
847 <https://doi.org/10.1016/j.ibiod.2006.01.003>, 2006.

848 Miller, A.Z. Sanmartín, P., Pereira-Pardo, L., Dionísio, A., Saiz-Jimenez, C., Macedo, M.F., Prieto,  
849 B.: Bioreceptivity of building stones: A review, *Science of The Total Environment*, Volume

850 426, 1-12, <https://doi.org/10.1016/j.scitotenv.2012.03.026>, 2012

851 Monte, M Del, Sabbioni, C.: Chemical and bioweathering of an historical building: Reggio Emilia  
852 Cathedral. *Science of The Total Environment*, 50: 165-182, [https://doi.org/10.1016/0048-9697\(86\)90358-X](https://doi.org/10.1016/0048-9697(86)90358-X), 1986

853

854 Moropoulou, A, Bisbikou, K, Torfs, K, Van Grieken, R, Zerza, F, Macri, F.: Origin and growth of  
855 weathering crusts on ancient marbles in industrial atmosphere. *Atmospheric Environment*,  
856 32(6): 967-982, [https://doi.org/10.1016/S1352-2310\(97\)00129-5](https://doi.org/10.1016/S1352-2310(97)00129-5), 1998

857 Pinna, D, Galeotti, M, Perito, B, Daly, G, Salvadori, B.: In situ long-term monitoring of  
858 recolonization by fungi and lichens after innovative and traditional conservative treatments  
859 of archaeological stones in Fiesole (Italy). *International Biodeterioration & Biodegradation*,  
860 Volume 132, 49-58, <https://doi.org/10.1016/j.ibiod.2018.05.003>, 2018

861 Pinna, D.: *Coping with Biological Growth on Stone Heritage Objects: Methods, Products,  
862 Applications, and Perspectives* (1st ed.). Apple Academic Press.  
863 <https://doi.org/10.1201/9781315365510>, 2017

864 Praderio, G., Schiraldi, A., Sorlini, C., Stassi, A., Zanardini, E.: Microbiological and calorimetric  
865 investigations on degraded marbles from the Cà d'Oro facade (Venice). *Thermochimica Acta*,  
866 227: 205-213. [https://doi.org/10.1016/0040-6031\(93\)80263-A](https://doi.org/10.1016/0040-6031(93)80263-A), 1993.

867 Qu, S.: The research on the weathering mechanism and weathering degree evaluation system of  
868 marble relics in Beijing. Master's Thesis. Beijing: Beijing University of Chemical Technology.  
869 1-140, 2018.

870 Santo, A., P., Agostini, B., Cuzman, O., A., Michelozzi, M., Salvatici, T., Perito, B.: Essential oils  
871 to contrast biodeterioration of the external marble of Florence Cathedral, *Science of The Total  
872 Environment*, V. 877, <https://doi.org/10.1016/j.scitotenv.2023.162913>, 2023,

873 Scheerer, S., Ortega-Morales, O., & Gaylarde, C.: Microbial deterioration of stone monuments—an  
874 updated overview. *Advances in Applied Microbiology*, 66, 97-139,  
875 [https://doi.org/10.1016/S0065-2164\(08\)00805-8](https://doi.org/10.1016/S0065-2164(08)00805-8), 2009

876 Tian, Y., Zhang, J., Song, L., Bao, H.: A study on aerial algae communities on the surface of  
877 carbonate rock of the Yunnan stone forest. *Carsologica Sinica*, (03): 39-47, 2003.

878 Tian, Y., Zhang, J., Song, L., Bao, H.: A Study on Aerial Cyanophyta (Cyanobacteria) on the Surface  
879 of Carbonate Rock in Yunnan Stone Forest, Yunnan Province, China. *Acta Ecologica Sinica*,

880 (11): 1793-1802+2020-2022, 2002.

881 Tian, Y., Zhang, J., Song, L., Bao, H.: The role of aerial algae in the formation of the landscape of  
882 the Yunnan Stone Forest, Yunnan Province, China. *Science in China, Series D: Earth Sciences*,  
883 47(9): 846-864., 2004.

884 Timoncini, A., Costantini, F., Bernardi, E., Martini, C., Mugnai, F., Mancuso, F. P., Sassoni, E.,  
885 Ospitali, F., & Chiavari, C.: Insight on bacteria communities in outdoor bronze and marble  
886 artefacts in a changing environment. *Science of the Total Environment*, 850,  
887 <https://doi.org/10.1016/j.scitotenv.2022.157804>, 2022

888 Trovão, J., Portugal, A.: The impact of stone position and location on the microbiome of a marble  
889 statue. *The Microbe*, 2, 100040. <https://doi.org/10.1016/j.microb.2024.100040>, 2024

890 Venturi, S., Tassi, F., Cabassi, J. , Gioli, B. , Baronti, S., Vaselli, O., Caponi, C. , Vagnoli, C.  
891 Picchi, G., Zaldei, A., Magi, F., Miglietta, F. , Capecchiacci, F. : Seasonal and diurnal  
892 variations of greenhouse gases in Florence (Italy): Inferring sources and sinks from carbon  
893 isotopic ratios, *Science of The Total Environment*, Volume 698,  
894 <https://doi.org/10.1016/j.scitotenv.2019.134245>, 2020.

895 Wang, F, Fu, Y, Li, D, Huang, Y, Wei, S.: Study on the mechanism of the black crust formation on  
896 the ancient marble sculptures and the effect of pollution in Beijing area. *Helijon*, 8(9):  
897 e10442, 2022

898 Wang, S.: The characteristic analysis of surface deterioration and mechanism study on West Yellow  
899 Temple Stone heritage. Master's Thesis. Beijing: China University of Geosciences (Beijing). 1-  
900 57, 2010.

901 Warscheid, T., Braams, J.: Biodeterioration of stone: a review. *International Biodeterioration &*  
902 *Biodegradation*, 46(4): 343-368, [https://doi.org/10.1016/S0964-8305\(00\)00109-8](https://doi.org/10.1016/S0964-8305(00)00109-8), 2000

903 Wu, M., Liu, J.: Fangshan Dashiwo and Stone Quarrying for Ming Dynasty Palaces and Tombs in  
904 Beijing - Also on Stone Usage in Beijing's Imperial Construction Through Dynasties.  
905 Proceedings of the Palace Museum (First Volume). 253-262, 1996.

906 Wu, Y., Zhang, B., Zhang, J., Zhai, K., Luo, L.: Weathering Characteristics of White Marble Relics  
907 Around the Hall of Supreme Harmony (Taihe Dian) in the Forbidden City. *KSCE Journal of*  
908 *Civil Engineering*, 27(2): 794-804, <https://link.cnki.net/doi/10.1007/s12205-022-1108-z>  
909 2023.

910 Yang, X.: Study on Weathering mechanism of Beijing Marble. Master's Thesis. Beijing: China  
911 University of Geosciences (Beijing): 1-92, 2016.

912 Ye, J., Zhang, Z.: Correlation Study of Physical and Mechanical Parameters of Beijing Marble.  
913 Journal of Engineering Geology, 27 (3): 532-538.  
914 <https://link.cnki.net/doi/10.13544/j.cnki.jeg.2018-102>, 2019.

915 Zhang, G.: Research on the weathering mechanism and Protection technology of spalling disease of  
916 Marble relics in Beijing. Master's Thesis. Beijing: Beijing University of Chemical Technology.  
917 1-77. <https://link.cnki.net/doi/10.26939/d.cnki.gbhgu.2022.000801>, 2022.

918 Zhang, T., Li, D., Zhang, Z.: Damage categories and deterioration mechanism of stone cultural relics  
919 of white marble in Beijing. Geotechnical Investigation & Surveying, 44 (11): 7-13, 2016.

920 Zhang, Z., Yang, X., Ye, F., et al.: Microscopic characteristics of petrography and discussion on  
921 weathering mechanism of Fangshan marble in Beijing. Journal of Engineering Geology, 23  
922 (02): 279-286. <https://link.cnki.net/doi/10.13544/j.cnki.jeg.2015.02.013>, 2015.

923 Zheng, L., Li, K., Wang, J., Li, L., Wang, Y., Wang, M.: Investigations on the surface deterioration  
924 process and mechanisms of white marble. Construction and Building Materials, 472: 140844,  
925 <https://link.cnki.net/doi/10.1016/j.conbuildmat.2025.140844>, 2025

926 Zhu, H.: Freshwater Algae in China (Volume 2, Orders Chroococcales). Beijing: Science Press. 1-  
927 105, 1991.

928

929

930

931